

Hot-spring inputs and climate drive dynamic shifts in archaeal communities in Lake Magadi, Kenya Rift Valley

Evan R. Collins¹, Troy M. Ferland², Isla S. Castañeda³, R. Bernhart Owen⁴, Tim K. Lowenstein⁵,
†Andrew S. Cohen⁶, Robin W. Renaut⁷, Molly D. O’Beirne¹, Josef P. Werne¹

5 ¹Department of Geology and Environmental Science, University of Pittsburgh, Pittsburgh, PA, 15213, United States

²Lamont-Doherty Earth Observatory, Columbia University, Palisades, NY, 10964, United States

³Department of Earth, Geographic and Climate Sciences, University of Massachusetts Amherst, Amherst, MA, 01003, United States

⁴Department of Geography, Hong Kong Baptist University, Kowloon Tong, Hong Kong

10 ⁵Department of Geological Sciences, State University of New York, Binghamton, NY 13902, United States

⁶Department of Geosciences, The University of Arizona, Tucson, AZ 85721, United States

⁷Department of Geological Sciences, University of Saskatchewan, Saskatoon, SK S7N 5E2, Canada

Correspondence to: Evan R. Collins (erc92@pitt.edu/ecollins452@gmail.com)

Abstract. The Methane Index (MI) is an organic geochemical index that uses isoprenoid glycerol dialkyl 15 glycerol tetraethers (GDGTs) as a proxy for methane cycling. Here, we report results from sediments in core MAG14-2A that span almost 500 ka in Lake Magadi, Kenya. The deposits show abrupt shifts between high and low MI values through calcareous, tuffaceous and zeolitic silts. The MI switches “off” (MI < 0.2) and “on” (MI > 0.5) through the core with bulk organic matter enriched in ^{13}C during “MI-off” periods (~ -18‰) in the upper part of the core, whereas ^{13}C is lower (-22 to -25‰) in lower parts of 20 the sedimentary sequence. Sediments deposited when the MI switches “on” showed $\delta^{13}\text{C}_{\text{OM}}$ values as low as -89.4 ‰, but most were within the range of -28 to -30‰, which is consistent with contributions from methanogens rather than methanotrophs. Thus, the likely source of these high MI values in Lake 25 Magadi is methanogenic archaea. Our results show that hydrothermal inputs of bicarbonate-rich waters into Lake Magadi combined with further evaporative concentration cause a shift in the dominant archaeal communities, alternating between two stable states.

1 Introduction

Life thrives in East African soda lakes and has been the subject of modern studies of both prokaryotic and eukaryotic organisms, but few have studied their sediments over geologic timescales (Schagerl, 2016 and

chapters therein). Soda lakes represent $\sim 18,500$ km 2 in East Africa (calculated from values in Melack and MacIntyre, 2016). When compared to the three largest African freshwater lakes (lakes Victoria, Tanganyika, and Malawi), these soda lakes account for $\sim 13\%$ of the total lake-surface area in East Africa. A survey of microbial isolate diversity in East African lakes found evidence for cyanobacterial and archaeal primary producers with both oxygenic and anoxygenic phototrophs among the microbial population (Grant and Jones, 2016). Unique aerobic and anaerobic heterotrophs that use a variety of 35 electron donors, including sulfur, sulfate, nitrite, carbon dioxide, and methane, were also identified (Grant and Jones, 2016, and sources therein). Many thermophilic archaea and bacteria isolates were also observed near hot-spring outflows (Grant and Jones, 2016).

Saline alkaline (soda) lakes in the East African Rift often become stratified meromictic water bodies with 40 a dense monimolimnion below a chemocline (Melack and MacIntyre, 2016). Oxygen rarely penetrates the monimolimnion waters, and as a result, anaerobic bacteria and archaea dominate the bottom waters and sediments. Remineralizing organic matter from the upper water column (mixolimnion) supports the microbes and the anaerobic oxidation of methane (AOM). Methane-oxidizing microbes, specifically 45 archaeal anaerobic methane-oxidizers (ANME), are coupled to sulfate-reducing bacteria in a microbial consortium (Boetius et al., 2000; Hinrichs and Boetius, 2002; Werne et al., 2004). ANME mediate methane levels in freshwater and soda lakes and in modern oceanic systems, and account for approximately 90% of methane consumed through AOM (Egger et al., 2018). Rates of methane consumption differ by environment and type of ANME, with global freshwater systems ranging from 1 to 1×10^5 nmol methane L $^{-1}$ day $^{-1}$ consumed (Martinez-Cruz et al., 2018). Although soda lakes have been 50 less studied, consumption rates as high as 1.6×10^4 nmol methane L $^{-1}$ day $^{-1}$ have been observed in freshwater Lake Kivu (Roland et al., 2018). Tracking AOM over geologic time periods is important because methane release from tropical wetlands was concomitant with the end of glacial conditions in Europe and is poorly constrained (DeMenocal et al., 2000; Riddell-Young et al., 2023). Additionally, 55 large methane releases might have been partly responsible for the Permo-Triassic mass-extinction event (Berner, 2002).

Over geologic time, it is possible to gauge periods of increased methane oxidation, as shown by Zhang et al. (2011) in oceanic systems by using a ratio of archaeal GDGT lipids (de Rosa et al., 1977; Langworthy, 1977). The ratio, as described by Zhang et al. (2011), is known as the methane index (MI), which uses 60 GDGTs produced predominantly by Euryarchaeal ANME. The MI has been used to discern methanotrophy using the assumption that benthic methanotrophic Euryarchaeota preferentially produce GDGT-1, -2, and -3, and that GDGTs crenarchaeol (cren) and crenarchaeol' (cren') are thought to come from Thaumarchaeota and Crenarchaeota, which are part of the TACK superphylum, typically found in the upper water column (Sinninghe Damsté et al., 2002; Pitcher et al., 2009; Zhang et al., 2011). Currently, 65 the newly suggested names in the Genome Taxonomy Database for Thaumarchaeota and Crenarchaeota are Nitrososphaerota and Thermoproteota, respectively (Oren and Garrity, 2021; Rinke et al., 2021), which are used in this paper.

Kim and Zhang (2023) have shown a qualitative and quantitative relationship between the MI and 70 methanotrophy in deep time, namely from the late Oligocene to the early Miocene. Kim and Zhang (2023) showed that the MI is applicable to AOM, with other biomarkers co-occurring in high-MI intervals representative of not only the Group I consortium of anaerobic methanotrophs (ANME) that produce GDGTs, but also of Group 2 and Group 3 consortia (ANME-2 and ANME-3 respectively). Until now, no 75 studies have directly applied the MI to sediments in African soda lakes despite evidence for AOM in modern soda lakes. Combined with MI values, other methane-related indices are used here to interpret methanogenesis and methanotrophy related to AOM. Previous studies have used GDGT-0 and GDGT-2 ratioed to the GDGT crenarchaeol value, which was originally thought to only be produced by mesophilic Thermoproteota (Blaga et al., 2009; Weijers et al., 2012). However, the optimum temperature for 80 crenarchaeol production is closer to 40-45 °C (Zhang et al., 2006). Blaga et al. (2009) found that methanogens predominantly produced GDGT-0, whereas Weijers et al. (2011) showed that methanotrophic archaea predominantly produce GDGT-2.

Lake Magadi (Kenya) is a sulfate-limited lake, and therefore, methanogenesis and methanotrophy may co-occur without suppression of the higher energy yield of sulfate reduction (Nijaguna, 2006; Sorokin et

85 al., 2007; Deocampo and Renaut, 2016; Lameck et al., 2023). Here, we document evidence of methane cycling in Lake Magadi using archaeal isoprenoid GDGT lipid biomarkers. Environmental influences on archaeal community composition included precipitation/evaporation fluctuations and variations in hydrothermal activity, the latter often related to contemporary tectonics. This study leverages four methane-related indices: (1) the MI; (2) the %GDGT-0/crenarchaeol; (3) %GDGT-2/crenarchaeol; and
90 (4) the ratio of isoprenoid GDGTs [2]/[3] (hereafter, [2]/[3]) to understand methane cycling in recent and ancient lacustrine sediments. Two distinct communities were found using a combination of the MI and ratios of GDGT-0 and GDGT-2, normalized to crenarchaeol. Intervals of high methanotrophy, as evidenced by MI and %GDGT-2/crenarchaeol, were related to an equally high proportion of methanogens, while in periods when crenarchaeol was dominant, the methane indices were low.

95 2 Materials and methods

2.1 Study locations and sampling

Modern Lake Magadi is a seasonally flooded, saline alkaline pan composed of bedded trona ($[\text{Na}_3(\text{CO}_3)(\text{HCO}_3) \cdot 2\text{H}_2\text{O}]$) located in the southern Kenya Rift near the border with Tanzania (Baker, 1958; Eugster, 1980). Its elevation is approximately 600–605 m above sea level (asl), and it has a
100 maximum depth during the rainy season of a few decimeters to ~1 m (Fig. 1; Renaut and Owen, 2023). Although Lake Magadi is situated near the equator, it lies in a rain shadow. Consequently, today it has a large moisture deficit (2400 mm evaporation versus 500 mm precipitation annually: Damnati and Taieb, 1995).

105 The modern alkaline lake is fed by ephemeral streams and alkaline hot springs (up to 86°C at adjacent Nasikie Engida), distributed along faults around the shoreline (Baker, 1958; Crane, 1981; Allen et al., 1989; Renaut and Owen, 2023). Former high-level shorelines are preserved as coarse clastic sediments and locally as stromatolites around the lake. These vary in age and record lakes of different depths during the Quaternary. Outcrops of sediments relevant to this study and situated near Lake Magadi are the
110 Oloronga Beds and the Green Beds. The chert-bearing Oloronga Beds in outcrop were lain down between

~ 800 and 300 ka, with cores extending this back to 1 Ma (Owen et al., 2019). Green Beds outcrops include abundant chert and have been variably dated between 191 and 40 ka (Behr and Röhricht, 2000; Owen et al., 2019) with cores suggesting a range from 380 to 105 ka (Owen et al., 2019). The High Magadi Beds were deposited between ~25 and 9 ka (Fairhead et al., 1972; Goetz and Hillaire-Marcel, 115 Williamson et al., 1993; Behr and Röhricht, 2000; Owen et al., 2019; Reinhardt et al., 2019). Calcrete commonly caps the Oloronga Beds (Eugster, 1980), but fluvial erosion locally scoured those sediments before the Green Beds were laid down (Renaut and Owen, 2023).

120 Lake Magadi was cored as part of the *Hominin Sites and Paleolakes Drilling Project* (HSPDP) in June 2014 to further our understanding of the paleoenvironments in the East African Rift Valley and to better contextualize hominin remains and artifacts, and to understand possible environmental influences on hominin evolution and migration (Cohen et al., 2016). A 197.4-meter core (MAG-14-2A) was drilled in the northern end of Lake Magadi ($1^{\circ}51'5.76''$ S $36^{\circ}16'45.84''$ E; Owen et al., 2019). In total, 107.7 m of sediments were recovered, with an overall core recovery of 55.4% (Cohen et al., 2016). Here, we use the 125 age model from Owen et al. (2019). The core ranges from the modern trona surface (0 ka) to the Magadi Trachyte basement, dated to ~ 1 Ma at the core site (Owen et al., 2019). Cores were sampled in 2016 during the initial core description at the Continental Scientific Drilling Facility (CSD, formerly LacCore) at the University of Minnesota, Minneapolis. Altogether, 61 samples, covering the period from 456 ka to 14.9 ka (Table S1), were collected and freeze-dried from dark brown to black silty clay intervals. Based 130 on their color, these samples were expected to have a high total organic carbon that would yield the highest quantity of biomarkers for our study. The non-ideal sampling strategy is due to poor core recovery.

135 Over the past million years, Lake Magadi has varied from swampy fresh water bodies to a large fresh to mildly saline lake that was continuously fed by rivers and groundwater, to smaller hypersaline lakes bounded by the Magadi grabens that dried to trona pans partly fed by hot springs (Owen et al., 2019; Renaut and Owen, 2023). From 545 to 380 ka the Magadi catchment progressively changed to a more arid condition with the palaeolake marked by abundant calcareous, organic-rich sediments (Owen et al., 2019). Periodic freshwater inundation occurred from 380 to 105 ka into a highly saline, alkaline lake that

140 accumulated minor calcite and magnesium-rich calcite at lake margins. Ash that fell into this waterbody reacted to form a variety of zeolites with anoxic, sulfate-rich bottom-water brines subjected to microbial sulfate reduction (Owen et al., 2019; Deocampo et al., 2022). The most recent phases of the lake (105 to 0 ka) were more evaporatively enriched, with abundant trona and minor nahcolite. Well-preserved diatoms in sediments deposited after ~500 ka suggest very high aqueous silica in the paleolake in order to explain the preservation of their frustules under highly alkaline conditions, which may reflect strong 145 evaporative concentration of silica-rich hydrothermal inflows (Owen et al., 2019).

2.2 GDGT and bulk organic preparation and analysis

2.2.1 Lipid extraction

150 To obtain a total lipid extract (TLE), 61 samples from Lake Magadi were freeze dried and homogenized and ca. 5–10 g of sediment were ultrasonically extracted with 2:1 DCM:MeOH. The TLE for each sample was treated with activated copper shot to remove elemental sulfur. The TLEs were then separated into three fractions (apolar (AP), polar one (P1), and polar two (P2)) using activated alumina via short column chromatography. The AP fraction was eluted with 4 mL of 9:1 Hexane (Hex):DCM (v/v), the P1 fraction with 4 ml 1:1 DCM:MeOH, and the P2 fraction with 4 ml MeOH. The P1 fractions were dried down and 155 re-dissolved in 99:1 Hex:Isopropanol (IPA) (v/v) and filtered through a 0.45 μ m 4 mm diameter PTFE filter prior to GDGT analysis.

2.2.2 Bulk organic $\delta^{13}\text{C}_{\text{OM}}$ analysis

160 Samples were subsampled from the same intervals as organic biomarkers for bulk organic carbon isotope analysis. Powdered sediment samples were weighed in silver capsules and carbonates were removed by adding 5% HCl in four-hour increments. Samples were analyzed on a Costech Elemental Analyzer coupled to a ThermoFinnigan Delta V Plus isotope ratio monitoring mass spectrometer (IRMS). Samples are reported as per mil (‰) deviations from the Vienna Pee Dee Belemnite (VPDB) standard in conventional delta notation.

2.3 GDGT preparation and analysis

165 2.3.1 GDGT analysis

Polar samples from Lake Magadi were analyzed for core lipid isoprenoid glycerol dialkyl glycerol tetraethers (iso-GDGTs) at the University of Massachusetts Amherst on an Agilent 1260 series high performance liquid chromatograph (HPLC; Fig. S1) in tandem with an Agilent 6120 series single quadrupole mass selective detector (MSD). Compounds were ionized using atmospheric pressure chemical ionization (APCI). The columns used for GDGT separation were a pre-column guard followed by two ultra-high performance liquid chromatography (UHPLC) silica columns (BEH HILIC, 2.1x150 mm, 1.7 μ m, Waters) connected in series and kept at 30 °C. Elution solvents followed Hopmans et al. (2016) using a flow rate of 0.2 mL min⁻¹. Two solvent mixtures, hexane (A) and 9:1 Hex:IPA (B), were eluted isocratically for 25 minutes with 18% B, a linear gradient to 35% B in 25 minutes, a second linear gradient to 100% B in 30 minutes.

175 2.3.2 GDGT indices

Several different ratios based on the relative abundance of different isoprenoid GDGTs have been developed to determine their source(s). The methane index (MI) is defined by Zhang et al. (2011) and is calculated as in Eq. (1):

180

$$MI = \frac{GDGT-1+GDGT-2+GDGT-3}{GDGT-1+GDGT-2+GDGT-3+Cren+Cren'} \quad (1)$$

MI values range between 0 and 1 with values > 0.5 considered to be derived from methanotrophic communities and values < 0.3 considered normal sedimentary conditions (Zhang et al., 2011). These 185 proposed ranges from Zhang et al. (2011) were derived from GDGTs found in marine sediments, so the cutoff values for methanotrophy may differ in lacustrine sediments, particularly those in saline, alkaline environments.

The ratio of GDGT-2 / crenarchaeol (%GDGT-2/cren) also indicates methanotrophy (values > 0.2),
190 specifically methanotrophy associated with sulfate-methane transition zones (Weijers et al., 2011). These values were normalized and converted to percentages so that the numbers produced could be contextualized with the other indices used (Eq. 2). As a result, %GDGT-2/cren contributions greater than 33% will be considered methanotrophic signals.

195
$$\%GDGT - 2/cren = \frac{[GDGT-2]}{[GDGT-2]+[Cren]} * 100 \quad (2)$$

Methanogenic inputs are calculated similarly to Eq. 2 above using GDGT-0 in place of GDGT-2. Blaga et al. (2009) found that values of GDGT-0 / (GDGT-0 + cren) > 2 are associated with methanogenic archaeal communities in a study of freshwater lakes. Similarly, in a study of Eocene marine sediments,
200 Inglis et al. (2015) normalized the equation and converted it to a percentage, a convention we follow (Eq. 3). They found that contributions from methanogens were indicated by values greater than 67%.

$$\%GDGT - 0/cren = \frac{[GDGT-0]}{[GDGT-0]+[Cren]} * 100 \quad (3)$$

205 The GDGT-2 / GDGT-3 ([2]/[3]) index is used here to describe both mesophilic environments as well as environments with high MI values. Rattanasriampaipong et al. (2022) found that differences in [2]/[3] are linked to distinct archaeal communities whereby low values of [2]/[3] (ca. 0.55) are observed in thermophilic cultures while elevated values are indicative of hot spring mats (ca. 1.00), shallow aerobic ammonia-oxidizing archaea (AOA; ca. 1.16), or archaea in suspended particulate matter (ca. 2.52). This
210 is the same version described in Rattanasriampaipong et al. (2022) (Eq. 4).

$$[2]/[3] = [GDGT - 2]/[GDGT - 3] \quad (4)$$

2.4 Bulk geochemistry

215 Bulk geochemical data and core descriptions from Owen et al. (2019, 2024) were used to interpret hot spring influences in the intervals of focus in the sediment core (designated as intervals 1, 3, and 5 in the results and discussion sections). They attributed rare earth element (REE) anomalies to increased lake alkalinity, which reflected increased evaporation and the development of highly saline, alkaline lakes and possibly increased hydrothermal/fluvial inflow ratios. All statistical analyses were performed using the
220 GraphPad Prism 10[©] software (<https://www.graphpad.com/>). Only the necessary data to determine relationships between the bulk geochemistry of REEs (La, Ce, Nd, Sm, Eu, Yb, Lu) and methane indices (MI, %GDGT-0/cren, %GDGT-2/cren, and [2]/[3]) were imported. The data was tested for normality via the built-in "Normality and Lognormality Tests" function in Graph Pad[©]. Tests yielded lognormal distributions of each dataset and found the data to be non-normally distributed. Additionally, pyrite cubes
225 were visually assessed without the use of a microscope during the initial core description and during organic extractions, however, no smear slides were collected and assessed.

2.4.1 Principal component analysis (PCA)

For the PCA, the imported data were analyzed using the built-in PCA function in GraphPad[©]. The data were standardized, which scaled the data to a mean of 0 and a standard deviation of 1. The principal
230 components were selected based on their eigenvalues using the Kaiser Rule, which selects eigenvalues greater than 1.0. Principal components 1 and 2 explained 58.0% of the variance in the data.

2.4.2 Correlation matrix

The correlation matrix was performed using the built-in function in GraphPad[©]. Because the data were non-normally distributed, the nonparametric Spearman correlation was chosen over the Pearson
235 correlation. An r value was computed for every pair of Y datasets using the default two-tailed option at a 95% confidence interval.

3 Results

3.1 GDGT lipid variability

Samples are split into six intervals (1-6) based partly on their fractional abundances of GDGT-0 and cren as well as their MI values: (1) 35.67 to 32.61 m; ca. 17.7 to 14.9 ka, (2) 67.81 to 43.51 m; ca. 129 to 38.9 ka (3) 86.06 to 70.78 m; ca. 197 to 149 ka, (4) 96.38 to 94.91 m; ca. 318 to 315 ka, (5) 104.10 to 103.16 m; ca. 324 to 323 ka, and (6) 130.21 to 119.64 m; ca. 456 to 391 ka (Table S1).

In each of the intervals of the core, MI, %GDGT-0/cren, and %GDGT-2/cren values oscillate between high and low values, changing abruptly from one interval to the next (Table S1). The methanotrophic (%GDGT-2/cren) and the methanogenic (%GDGT-0/cren) indices track similarly to MI values; that is, when values of MI are high, so are the other two indices. It should be noted that there are some large gaps in sampling between intervals in the core due to our sampling regime (i.e. targeting intervals with high apparent organic matter based on darker silty matrix). Interval 1 is characterized by a higher proportion of cren and lower overall index values. The %GDGT-0/cren index averages 36.3 % ($\pm 0.09\%$) in this interval while the %GDGT-2/cren index averages 10.6 % ($\pm 0.05\%$; Fig. 2). The MI in this interval is correspondingly low with an average of 0.25 (± 0.07), well below the MI = 0.5 cutoff range for methanotroph-impacted communities. As such, this interval could be used for the [2]/[3] index; values averaged 2.1 (± 1.02). Interval 2 has much higher values for each of these indices, where the average %GDGT-0/cren = 99.3 % ($\pm 0\%$) and the average %GDGT-2/cren = 93.6 % ($\pm 0.04\%$). MI values in Interval 2 are also high with an average of 0.96 (± 0.02). Of note, there is a large gap where no measurements were taken from 43.55 to 46.68 m (~9.7 kyr) as well as from 50.36 to 58.74 m (~32.5 kyr). Interval 3 averages for %GDGT-0/cren and %GDGT-2/cren are 54.3 ($\pm 0.27\%$) and 20.4 % ($\pm 0.26\%$), respectively. However, there is one anomalously high value at 77.32 m with %GDGT-0/cren and %GDGT-2/cren values at 99.6 and 93.8 % and an MI = 0.96. Excluding the high index value, the averages were lowered to 48.6 ($\pm 0.22\%$) and 11.2 % ($\pm 0.05\%$) for the %GDGT-0/cren and %GDGT-2/cren values and the MI average was lowered from 0.33 (± 0.23) to 0.26 (± 0.06). With the exclusion of 77.32 m, the [2]/[3] index averaged 1.5 (± 0.80) in this interval, lower than Interval 1. Interval 4 is characterized by high index values, with a similarly abrupt shift from low values. Averages of the %GDGT-0/cren and

265 %GDGT-2/cren are 98.1 ($\pm 0.04\%$) and 88.2 % ($\pm 7.41\%$) and an average MI of 0.92 (± 0.04); these
270 average index values are similarly high as compared to Interval 2. Interval 5 is a shift to lower overall
index values with averages of %GDGT-0/cren and %GDGT-2/cren at 40.1 ($\pm 0.17\%$) and 9.2 % ($\pm 0.03\%$) and an average MI of 0.22 (± 0.05). Finally, Interval 6 shows a period in the core with high index
values throughout. Averages of %GDGT-0/cren, %GDGT-2/cren, and MI are 97.6 % ($\pm 0.03\%$), 89.4 %
($\pm 0.08\%$), and 0.95 (± 0.05), respectively.

3.2 Bulk $\delta^{13}\text{COM}$ values

Bulk $\delta^{13}\text{COM}$ values follow a similar pattern to the indices described in section 3.1, that is the values
275 oscillate between high and low values between intervals. Samples in Interval 1 ranged from -21.9 to -16.8
 \textperthousand and had an average $\delta^{13}\text{COM}$ value of -18.4 \textperthousand with respect to VPDB. Interval 2 samples had the most
 ^{13}C -depleted values in all sampled intervals, ranging from -89.4 to -24.7 \textperthousand with an average of -35.1 \textperthousand
and excluding the three outlier values (-48.1, -64.2, and -89.4 \textperthousand), the Interval 2 average was -28.2 \textperthousand . In
Interval 3, the $\delta^{13}\text{COM}$ had a narrower range from -24.4 to -21.4 \textperthousand and an average of -22.5 \textperthousand . A lighter
signal from Interval 4 yielded a narrow range of values from -27.0 to -25.4 \textperthousand averaging -26.0 \textperthousand . Interval
280 5 had slightly heavier values ranging from -25.0 to -18.1 \textperthousand with an average of -22.1 \textperthousand . Lastly, Interval
6 had depleted $\delta^{13}\text{COM}$ values similar to intervals 2 and 4, with a range of -28.2 to -22.1 \textperthousand and an average
of -25.2 \textperthousand . Analytical reproducibility of duplicate runs was better than $\pm 0.15\text{\textperthousand}$ VPDB.

3.3 Bulk geochemistry

Both a PCA and correlation matrix were performed using the MI, Ca/Na, %GDGT-0/cren, %GDGT-
2/cren, and [2]/[3] to compare to the REEs La, Ce, Nd, Sm, Eu, Tb, Yb, and Lu (Fig. 3). Increased values
285 of REEs are characteristic of sodic systems influenced by hydrothermal springs, such as Mono Lake in
California and this system (Johannesson and Lyons, 1994; Owen et al., 2019). Additionally, the Ca/Na is
a proxy for the proportion of hydrothermal inflow to Lake Magadi such that a higher Ca/Na indicates
more freshwater input, while a lower Ca/Na indicates a higher proportion of hydrothermal water.

290 A PCA (Fig. 4a) and non-parametric Spearman correlation matrix (Fig. 4b) were performed to quantify the relationship between REEs, MI, Ca/Na and [2]/[3]. The PCA showed that Ca/Na loaded positively on PC1 and PC2 and each of the methane indices loaded positively on PC1 and negatively on PC2. The REE La loaded positively on PC2 and negatively on PC1 while the REEs Ce, Nd, Sm, Eu, Yb, and Lu loaded negatively on PCs 1 and 2. This indicates a negative relationship between the negatively loaded REEs 295 and a high Ca/Na. Similarly, the correlation matrix of REEs and methane indices showed a negative relationship between each index and REE, except for the relationship of [2]/[3] and Nd ($r=0.02$) and %GDGT-2/crem ($r=-0.04$), which showed no observable linear trend. The REEs and methane indices did not load on the same PC axis showing that there was also not a nonlinear trend associated with the REEs and methane indices.

300 4 Discussion

4.1 Lake Magadi archaeal community shifts

The abrupt changes in isoprenoid GDGT-based indices in the sediment record of Lake Magadi indicate shifts in the archaeal communities present (Fig. 2). Shifts between two distinct communities were inferred using a combination of the Methane Index (MI) and ratios of GDGT-0 and GDGT-2 normalized to 305 crenarchaeol (Eqs. 2 and 3). We denote these shifts as either “MI-on periods”, characterized by $MI > 0.5$ during intervals 2, 4, and 6, and “MI-off periods”, characterized by $MI < 0.5$ during intervals 1, 3, and 5. Oscillations between these two states are discussed in detail in the following sections.

4.1.1 MI-on periods

In Lake Magadi, during the MI-on periods (Fig. 2; Intervals 2, 4, and 6), the MI is persistently greater 310 than 0.83 and displays more ^{13}C -depleted $\delta^{13}\text{C}_{\text{OM}}$ values compared to MI-off periods, indicating periods of enhanced methane cycling. AOM is a likely mode of methane cycling in Interval 6 as well as parts of Interval 2 because SRB and AOM archaea live in a consortium together at the sulfate methane transition zone, or SMTZ (Boetius et al., 2000; Hinrichs and Boetius, 2002; Werne et al., 2004). Thus, in intervals 315 of the Magadi core where a SMTZ is suspected, such as in parts of Interval 2 and most of Intervals 4 and 6, there should be an increase in indices related to methanotrophy such as high MI and %GDGT-2/cren

(Weijers et al., 2011). Additionally, whereas methanogens and methanotrophs appear to be present in a consortium based on both the methane indices as well as bulk $\delta^{13}\text{C}_{\text{OM}}$, the majority of the contributions are coming from methanogens, as seen in the ternary plot in Fig. 5. This may seem counter-intuitive as the MI has been typically used to describe samples exhibiting a high predilection towards methanotrophy, 320 but a high MI value does not necessarily exclude methanogenesis and conversely neither does a low MI, rather the low MI value suggests a predominance of Thermoproteota over Euryarchaeota (Zhang et al., 2011). High %GDGT-0/cren and %GDGT-2/cren index values in Intervals 2, 4, and 6 (Fig. 2) show that methanogenesis is co-occurring with AOM. The [2]/[3] index is also useful in understanding the proportion of methanotrophs in sediments, even in intervals with high MI values like those discussed 325 herein (Table S1; Fig. 2). Values of the GDGT [2]/[3] ratio track nearly identically to the MI values (Fig. 2), indicating that the MI is influenced by GDGT-2, which is characteristic of methanotrophs (Pancost et al., 2001; Schouten et al., 2003; Zhang et al., 2011).

Typically, methanogenesis in sulfate-rich systems is suppressed in favor of sulfate reduction caused by 330 competition for both H_2 and organic substrates (Fazi et al., 2021; Sorokin et al., 2015). However, reports of methanogenesis co-occurring with SRB have been noted when methanogens are using non-competitive substrates such as methanol, or when sulfate levels are low (Oremland et al., 1982; Giani et al., 1984 Hoehler et al., 2001; Bebout et al., 2004; Arp et al., 2008, 2012; Jahnke et al., 2008; Smith et al., 2008; Robertson et al., 2009). Furthermore, pyrite cubes are common and scattered through the intervals where 335 high index values are observed, indicating that there was a substrate for SRB, though it may have been in low concentration (Table S1). Thus, the combined evidence of pyrite in intervals with high GDGT-based indices (e.g. MI, %GDGT-0/cren, and %GDGT-2/cren [2]/[3]) indicates the presence of a SMTZ that supports AOM with the co-occurrence of methanogenesis.

340 Looking at Figure 5, it appears that GDGT-0 is the dominant GDGT compared to GDGT-2 and cren, indicating that this interval is likely methanogen-dominant rather than ANME dominant. Interval 2 (Figs. 2 and 5) of the Magadi core appears to be more influenced by methanogenesis than AOM, as seen in a high %GDGT-0/cren signal accompanied by a high %GDGT-2/cren signal, high [2]/[3] ratios, and a more

13C-depleted bulk $\delta^{13}\text{COM}$ signal (average = -35.1 ‰; median = -28.6 ‰). Values of bulk $\delta^{13}\text{COM}$ are
345 similarly 13C-depleted in AOM-dominant Euryarchaeotal systems ranging from active mud volcanoes (~27 ‰; ANME-1), a Danish freshwater lake (average ~-29.7‰; ANME-2), and the Sea of Galilee (~-30 ‰; ANME-2) in Israel (Lee et al., 2018; Norði et al., 2013; Sivan et al., 2011). At points where the bulk
δ¹³COM values are at their lowest (e.g., -89 ‰), they are accompanied by a lower %GDGT-2/cren at ca.
95 % and an elevated %GDGT-0/cren at > 99.5 %. This aligns with the literature as Summons et al.
350 (1998) reported $\delta^{13}\text{COM}$ values between -53.4 and -48.7 ‰ in the total lipid extract of methylotrophic
methanogens using non-competitive substrates in anoxic hypersaline environments. Furthermore, as these
waters are typically sulfate-limited, acetoclastic and/or hydrogenotrophic methanogenesis is likely
dominant when evidence for SRB is lacking (i.e., pyrite). Zhuang et al. (2016) performed compound-
355 specific isotope analysis on several archaeol compounds from the Orca Basin and found archaeol and
hydroxyarchaeol using H₂ or CO₂ (diagnostic of methanogens and methanotrophs) were relatively
depleted (ca. -80 to -60 ‰) compared to the bulk $\delta^{13}\text{COM}$ (ca. -22 ‰). Zhuang et al. (2016) concluded that
acetoclastic and/or hydrogenotrophic methanogenesis was unlikely due to high SO₄²⁻ concentrations in
the Orca Basin, which may be the case in Lake Magadi. In Interval 2, there is no evidence of visible pyrite
cubes and we did not have a priority at the time of sampling to check a thin section of each sample for
360 smaller pyrite aggregates. This indicates that other Euryarchaeotal communities may have different forms
of AOM occurring in the sediments. These other forms of AOM include nitrate/nitrite reduction and iron
coupled to AOM ('t Zandt et al., 2018). This is further bolstered by the evidence outlined by Kim and
Zhang (2023) that not only quantitatively linked AOM to high MI values, but also to non-Group I ANME
Euryarchaea because other non-GDGT producing ANME (e.g. ANME-2 and ANME-3) were shown to
365 co-exist with Group I ANME. In the intervals that are missing pyrite (i.e., most of Interval 2; see Table
S1; Ferland, 2017), the pyrite may have either been too small to see with the naked eye or the excess H₂S
could have been incorporated into the kerogen by reacting with labile organic matter. From 59.40 to 58.80
m, values of the bulk $\delta^{13}\text{COM}$ dip as low as -89.4 ‰ (Table S1; Fig. 2), which aligns well with
methanogenic archaeal biomass (Norði et al., 2013). However, as discussed above there is likely
370 acetoclastic and/or hydrogenotrophic methanogenesis co-occurring in these high index intervals and is

likely the dominant process where sulfate-dependent AOM is absent, and the sulfate-dependent AOM is likely replaced by coupling to either nitrate/nitrite or iron reduction.

Samples in Interval 4 (Table S1) of the Magadi core have high index values but no evidence for sulfate-dependent methanotrophy except for high MI values. This interval is thus interpreted as being methanogenic rather than methanotrophic. The abundance of pyrite in the four samples with low MI values (Table S1; 104.10 to 103.16 m), indicates sulfate reduction not linked to AOM. This is not observed in any other level of the core and a hypothesized series of reactions is described below, which may be linked to an abundance of SRB, anaerobic ammonium oxidizing (anammox) bacteria, and Thermoproteota (AOA) in the overlying water column. Due to periodic influxes of freshwater in Magadi, in addition to a permanent meromixis present in almost all samples in this study post 380 ka, the water column would have been oxic in the upper portion and anoxic below the chemocline. Freshwater pulses would have also brought nutrients to the lake such as ammonia (NH_4^+) and sulfate (SO_4^{2-}). The oxic portion of the water column would have supported microaerophilic AOA that oxidize NH_4^+ to nitrite (NO_2^-), which is then transported to the anoxic part of the water column (Straka et al., 2019). Here, anammox bacteria use excess NH_4^+ and NO_2^- from the AOA and convert these to N_2 . Excess SO_4^{2-} is simultaneously being used by SRB, creating HS^- that is reacting with iron species in the sediments and being buried as pyrite. Ladderane lipids characteristic of marine annamox bacteria (Jetten et al., 2009) were not studied in Magadi sediments. However, there is both 16S rRNA and lipid evidence for the production of ladderanes in hot springs in the western United States suggesting that annamox bacteria can persist in hot spring environments (Jaeschke et al., 2009). Additionally, Kambura et al. (2016) found evidence for *Planctomycetes* in both microbial mat and water samples surrounding the hot springs of Lake Magadi, lending credence to the hypothesis of AOA persisting in Lake Magadi. Without other lines of evidence, however, these are hypothetical reactions for explaining excess pyrite in the sediments without accompanying MI values. Nonetheless, this explanation has merit because of the high relative abundance of both crenarchaeol and cren'.

In nearly all of Interval 6 (Table S1), there is evidence for a higher proportion of methanotrophic archaea from 128.74 to 119.64 m (increased %GDGT-2/cren and [2]/[3]) and methanogenesis in the intervals 400 from 130.21 to 129.77 m (Table S1; higher %GDGT-0/cren compared to %GDGT-2/cren). Samples from 123.43 to 119.64 (Table S1) are of note because the [2]/[3] values are lower than the MI values whereas every other MI and [2]/[3] values align nearly 1:1. This is likely due to GDGT-2 not being the dominant control of the MI. While both %GDGT-0/cren and %GDGT-2/cren are equally high, there may be other factors in the water column exporting GDGT-2 to the sediments, possibly from deep-dwelling Group I.1b 405 Thermoproteota, although this is unlikely due to limitations of depth (Taylor et al., 2013). The 656 m paleoshoreline reported by Casanova (1986, 1987) and Casanova and Hillaire-Marcel (1987) would imply a maximum water depth of ~ 50 m during the Late Pleistocene (African Humid Period: AHP) based on present topography. However, sedimentary evidence for such a high paleoshoreline is not seen throughout the Magadi Basin. Earlier water depths are also unclear because accommodation space was changing as 410 the axial rift developed with faulting and subsidence (Owen et al., 2024). This is not deep enough (> 1 km) to support Group I.1b Thermoproteota per the constraints outlined in Taylor et al. (2013).

4.1.2 MI-off periods

In intervals characterized by low MI, %GDGT-0/cren and %GDGT-2/cren values (Fig. 2; MI-off intervals 415 are odd numbers highlighted in blue), the $\delta^{13}\text{C}_{\text{OM}}$ values are ^{13}C -enriched relative to those intervals characterized by higher index values (Fig. 2; MI-on). Since the methane cycling indices (%GDGT-0/cren and %GDGT-2/cren) are both predominantly influenced by the availability of crenarchaeol, MI-off periods are marked by increased production in crenarchaeol. Typically, crenarchaeol is produced in open ocean systems, freshwater lakes, and soils by the mesotrophic aerobic ammonium oxidizing phylum Nitrososphaerota. However, they can also be found in other environments, such as in hot spring mats 420 made by Thermoproteota (Pearson et al., 2004, 2008; Schouten et al., 2013). As Thermoproteota require oxygen to oxidize ammonium to nitrate, the increased presence of crenarchaeol in the MI-off intervals, therefore, suggests periods when conditions were more oxic, at least in the upper water column. The increase in crenarchaeol, as well as the low [2]/[3] index values, suggest that more Thermoproteota were present in Lake Magadi in those periods. As mentioned in Section 4.1.1, three groups of AOA are of

425 interest for interpreting which archaeal groups are found in low index intervals of Lake Magadi. Averages
of [2]/[3] from the global dataset in Rattanasriampaipong et al. (2022) are as follows: hot spring mats
(avg. = 1.00), shallow AOA cultures (avg. = 1.16), and shallow core tops (avg. = 2.64). Placing these on
a continuum, we can approximate the environment from [2]/[3] averages in Magadi, though it should be
noted that the shallow AOA and shallow core-top values in Rattanasriampaipong et al. (2022) are based
430 on marine core-tops, while the hot spring mats are based on terrestrial hot springs like those observed
around Lake Magadi (i.e. pH > 6.5).

Interval 1 captures a transition from a more arid East Africa to a wetter period at the onset of the African
Humid Period (AHP). During wetter periods, more allochthonous material is transported to the lake,
435 which includes vegetal remains that impact the overall bulk $\delta^{13}\text{COM}$ values. This allochthonous vegetation
enriches the overall bulk $\delta^{13}\text{COM}$ values more significantly than other intervals in the Magadi core.
Average values of bulk $\delta^{13}\text{COM}$ are -17.7 ‰ in Interval 1, which correspond to the $\delta^{13}\text{COM}$ values of
aquatic sedges mixed with a terrestrial signal of grassy woodland (Sikes, 1994; Reiffarth et al., 2016).
Pollen records in Lake Magadi indicate that a mixture of C4 grassy woodlands and C4 aquatic sedges
440 were predominant in the landscape that surrounded Lake Magadi at this time (Muiruri et al., 2021). In
agreement with the pollen record, the $\delta^{13}\text{COM}$ values likely record a mixture of C4 grasses and C4 sedges.
Similar $\delta^{13}\text{C}$ values were reported in C₂₁ to C₃₃ n-alkanes in equatorial regions of Cameroon, ranging
from -18.2 to -17.6‰ and recording the signals from C4 grasses and sedges (Garcin et al., 2014). This all
suggests that the bulk $\delta^{13}\text{COM}$ signal is dominated by terrestrial biomass, unlike other sections of the core,
445 and there does not appear to be a significant influence from the benthic microbial community (i.e.,
methane cyclers or SRB).

Values of the [2]/[3] index average 2.1 in Interval 1 with some values as high as 3.74 and 4.63 at 33.28
and 33.03 m, respectively (Table S1). The higher values are closer to what is captured from deep oceanic
450 suspended particulate matter (SPM) and deep ocean core-tops below the pycnocline, though caution
should be used when comparing lacustrine and oceanic sediments (Rattanasriampaipong et al., 2022). The
increase in %GDGT-0/cren (50.6 and 54.3 %; Table S1) and the slightly increased MI values (0.37 and

0.41; Table S1) imply that these samples were deposited in a deeper lacustrine environment. Evidence for a deeper paleolake at ~40 feet (~17–18 m) above the modern lakeshore (Baker, 1958) is also observed in 455 the High Magadi Formation (ca. 17.7 to 10.8 ka) indicating that there was fresh water flowing into the lake during the period of deposition in Interval 1, likely creating a fresher water cap on the meromictic Lake Magadi (Barker et al., 1991; Behr, 2002; Owen et al., 2019). However, excluding the high [2]/[3] index values in Interval 1, the average is 1.6, which is closer to the hot spring mats and shallow AOA cultures (Rattanasriampaipong et al., 2022). Likely, the higher [2]/[3] index values represent periods of 460 increased methanogenesis occurring in the sediments, with AOA input from the upper water column likely induced by proportional increases in the amount of hydrothermal inflow to the lake (Section 4.2.1). Fig. 4 shows that the Ca/Na is anti-correlated with REEs in both the PCA and correlation matrix. Since the proportion of Ca/Na decreases when REEs increase, we can say that statistically, when it is drier (and thus proportionately more hydrothermally influenced) the Ca/Na decreases, REE values increase, and the 465 methane indices are suppressed. In the periods of lower [2]/[3] values, the community is interpreted as being dominated by AOA and thermophilic AOA cultures (i.e., Thermoproteota; Rattanasriampaipong et al., 2022) and is further supported by high % cren and % cren'. Kumar et al. (2019) described similarly low [2]/[3] values in the water column of Lake Malawi that are akin to values observed in Lake Magadi in both Intervals 1 and 3. They found that values of a lower normalized [2] / [2+3], ranging from 0.55 to 470 0.59, in Lake Malawi were associated with the shallower Thermoproteota (Thaumarchaeota) Group I.1b. This is compared to higher values of [2] / [2+3] in the deeper dwelling Thermoproteota Group I.1a, which means that most samples in Interval 1 are likely sourced from Group I.1b (Kumar et al., 2019). Kumar et al. (2019) concluded that Group I.1b Thermoproteota were contributing to the lower [2] / [2+3] values, while the more deeply dwelling Group I.1a Thermoproteota were more prevalent in aphotic portions of 475 the water column (Kumar et al., 2019). The normalized [2] / [2+3] used by Kumar et al. (2019), with values ranging from 0.55 to 0.65, approximates values of [2]/[3] in the 1.30 to 1.65 range as described in this paper. More recently, Baxter et al. (2021) found that Thermoproteota I.1b are more prevalent in the upper oxygenated portion of the water column within the photic zone as evidenced by a higher relative abundance of crenarchaeol and lower relative abundance of GDGT-2. Thus, our interpretations of 480 thaumarchaeotal AOA in Lake Magadi sediments are consistent with data from Baxter et al. (2021) and

Kumar et al. (2019). This interpretation is consistent with Interval 1 being a period of proportionately more freshwater and HCO_3^- -rich hydrothermal input and a deeper lake overall, which would explain the accompanying increase in crenarchaeol.

485 Interval 3 [2]/[3] averages are lower overall (Table S1; avg. = 5.4), with only one outlying high value (ca. 77.32 m at a value of 36.7). Excluding this high index value, the [2]/[3] average drops to 1.5, which is closer to what is observed in shallow AOA cultures and hot spring mats. With most samples being closer to unity (i.e., [2]/[3] = 1.0), it is likely that hot springs had a greater influence on the community composition in these intervals. Samples that are closer to unity (70.78, 70.86, and 71.08 to 75.93 m) also 490 have a relatively ^{13}C -enriched $\delta^{13}\text{C}_{\text{OM}}$ values (avg. = -21.8‰) compared to samples with a higher [2]/[3]. Average isotope values in Interval 3 are between oceanic hydrothermal vents (avg. = -19.0 ‰) and terrestrial alkaline hot spring systems such as the Bison Pool hot spring in Yellowstone National Park (avg. = -24.9 ‰) (Shah et al., 2008; Schubotz et al., 2013). Since elevated amounts of GDGT-2 (i.e., relative abundance > 45%) are associated with Euryarchaeota, and values in Intervals 1, 3, and 5 are much 495 lower than 45% (Table S1), these intervals are likely dominated by Thermoproteotal AOA (Pancost et al., 2001; Turich et al., 2007; Taylor et al., 2013). Archaeal community composition in Intervals 1, 3, and 5 is independent of these external factors and is related to hydrothermal flows. This further supports the hot springs driving the lake archaeal community composition as there was less overall precipitation and the Thermoproteotal communities were more abundant during Intervals 1, 3, and 5. Lastly, Interval 5, which 500 only has 4 samples, has similarly low values of [2]/[3] (average = 1.4) like Intervals 1 and 3, which is likely indicative of Thermoproteotal AOA cultures.

4.2 The influence of hot spring/runoff ratios on the archaeal methane cycles

Hydrothermal fluids in the basin are rich in carbonate and bicarbonate as well as Na^+ ions, inferred to be a result of the weathering and alteration of trachytic (silica-rich) basement rock (Jones et al., 1977; Allen 505 et al., 1989), and mantle-derived CO_2 discharged mainly along faults (Lee et al., 2017; Muirhead et al.). Ca^{2+} and Mg^{2+} are also very low (Deocampo and Renaut, 2016). Renaut and Owen (2023) note that hydrothermal waters become important contributors to lake recharge during arid phases when fluvial

inflow declines. For example, Nasikie Engida, a small hypersaline lake northwest of Lake Magadi, is partly maintained today by hydrothermal inputs, with trona, nahcolite and zeolites accumulating during 510 dry periods when there is little or no fluvial inflow (DeCort et al., 2019; Renaut et al., 2020; Renaut and Owen, 2023). Magadi Core MAG14-2A lacks evidence for complete desiccation (e.g., mudcracks, soils, calcrete) and the lake appears to have retained surface waters through multiple drought episodes during the last million years (Owen et al., 2019). In contrast, separate lakes in the neighbouring Koora Basin (~10 km to the east), dried out many times, leading to soil formation in that basin (Owen et al., 2024).

515

Owen et al. (2019) also noted that during periods when highly saline, alkaline water dominated at Magadi, ash was zeolitized, REE patterns developed significant anomalies, and pyrite developed in anoxic/euxinic bottom waters of a meromictic lake. They also noted the excellent preservation of diatom opaline silica in highly alkaline lakes after about 540 ka, which suggests that very high levels of silica in lake water 520 preserved their frustules from dissolution. Hydrothermal springs at Magadi today contain high silica, but their waters require further evaporation to achieve concentrations that would preserve diatom silica under very high pH conditions. High silica concentrations brought about by strong evaporation in a lake maintained by spring inflows (meteoric or hydrothermal) may partly explain the abundant chert through the Magadi sedimentary sequence.

525

Proportional increases in hot-spring water during periods of increased aridity would have favoured the development of highly saline, alkaline waters with significant impacts on archaeal communities. Samples in Interval 6 represent a drier period when the lake area and volume had shrunk, partly due to tectonic influences (Owen et al., 2024), and lake floor anoxia was prevalent (Owen et al., 2019). Between ~380 530 and 105 ka (Fig. 2; Interval 5 through mid-Interval 2), the paleolake was frequently meromictic with a freshwater mixolimnion that supported freshwater planktonic diatoms while the saline monimolimnion and lake floor waters favoured alteration of ash to a variety of zeolites (e.g., erionite, phillipsite, clinoptilolite, analcime) (Owen et al., 2019). Similarly, from ~105 to 0 ka (Fig. 2; mid-Interval 2 through Interval 1) low Ca/Na, increased Br, and the abundant zeolite formation, indicates saline conditions. After 535 about 80 ka, tectonic adjustments and increasing aridity led to desiccation in the Koora Basin suggesting

that spring inflows were important in maintaining a hypersaline lake in the Magadi Basin, as they do today during dry seasons (Owen et al., 2019). Ca/Na ratios have steadily decreased over time, though not at a 1:1 rate, which aligns with methane index values and sudden increases of these indices. Fig. 4 shows that the Ca/Na and methane indices are statistically different from one another in both the correlation 540 matrix and PCA plot. In Fig. 4b, Ca/Na is loaded positively on PC1 and PC2, while the methane indices ([2]/[3], MI, %0/Cren, and %2/Cren) are loaded positively on PC1 and negatively on PC2. Furthermore, REE data also appear to reflect our MI-off and MI-on periods as the REEs are anticorrelated in the correlation matrix (Fig. 4b) and loaded on different PC axes (Fig. 4a). Consequently, we interpret the changes in salinity and alkalinity in the Magadi paleolakes as reflecting the impact of climate on 545 spring/runoff ratios into the Magadi Basin, which in turn have exerted significant impact on the archaeal communities through the last million years. Samples in the low-MI intervals (ca. 32.61–35.67, 70.78–75.93, and 103.2–104.1 m) likely reflect proportionally increased spring/runoff ratios at Magadi caused by increased evaporation and decreased precipitation in the surrounding landscape.

5. Conclusions

550 Sediments in Lake Magadi track the environmentally driven changes in archaeal communities over the past ~ 456 ka. Using the MI to track the predominantly archaeal inputs at Lake Magadi, we have observed sudden and distinct shifts between mixed communities of Euryarchaeotal methanogens and methanotrophs transitioning to mesophilic AOA Thermoproteota communities and back again. This shift is driven, in part, by moisture balances in the East African Rift, with wetter conditions periodically 555 causing freshwater floods into a saline lake to form a meromictic waterbody at Magadi, and with more archaea derived from the upper water column rather than the sediments, as evidenced by low MI, low [2]/[3], and relatively ^{13}C -enriched bulk $\delta^{13}\text{C}_{\text{OM}}$. Methane indices were typically higher during periods of reduced hydrothermal activity, indicating more Euryarchaeal communities, whereas Thermoproteota communities thrived during periods of higher hydrothermal activity. This is a clear relationship between 560 low MI values, spring/runoff ratios, lake salinity, alkalinity and the development of mesophilic Thermoproteota. This study is one of the first to examine methane cycling in a soda lake over geologic time and provides valuable insights into how variable these systems can be. Soda lakes are important

ecosystems for methane cyclers and should be studied more closely so that we can improve understanding of global methane contributions in the past, and constrain sources in the future.

565 **6. Acknowledgements**

We thank the Kenya National Council for Science and Technology (NCSTI) for granting research permits. Drilling and environmental permits were provided by the Kenya Ministry of Petroleum Mining and the National Environmental Management Authority of Kenya. We especially thank the National Environment Management Authority (NEMA). The Research Grants Council of Hong Kong provided support to 570 Richard Bernhart Owen. We give special thanks the local Magadi Township Maasai community for their approval of the project and Tata Chemicals Magadi for providing field support. DOSECC Exploration Services supervised drilling that was undertaken by Drilling and Prospecting International (DPI). We also thank the CSD facilities (University of Minnesota) for allowing us to store and log our cores at their repository. Drilling at Magadi for the Hominin Sites and Paleolakes Drilling Project (HSPDP) was funded 575 by ICDP and NSF grants (EAR-1123942, BCS-1241859, EAR-1338553). This is Publication #XXX of the Hominin Sites and Paleolakes Drilling Project.

REFERENCES

580 Allen, D. J., Darling, W. G., and Burgess, W. G.: Geothermics and hydrogeology of the southern part of the Kenya Rift Valley with emphasis on the Magadi-Nakuru area, *Brit. Geol. Surv. Res. Rep.*, SD/89/1, 1989.

Arp, G., Ostertag-Henning, C., Yuecekent, S., Reitner, J., and Thiel, V.: Methane-related microbial gypsum calcitization in stromatolites of a marine evaporative setting (Münster Formation, Upper 585 Jurassic, Hils Syncline, north Germany), *Sedimentology*, 55, 1227–1251, 2008.

Arp, G., Helms, G., Karlinska, K., Schumann, G., Reimer, A., Reitner, J., and Trichet, J.:

Photosynthesis versus exopolymer degradation in the formation of microbialites on the atoll of Kiritimati, Republic of Kiribati, Central Pacific, *Geomicrobiol. J.*, 29, 29–65, 2012.

Baker, B.H.: Geology of the Magadi area, *Geol. Surv. Kenya Rep.*, 42, 1958.

590 Barker, P., Gasse, F., Roberts, N., and Taieb, M.: Taphonomy and diagenesis in diatom assemblages; a Late Pleistocene palaeoecological study from Lake Magadi, Kenya, *Hydrobiologia*, 214, 267–272. 1991.

Bauersachs, T., Schwark, L.: Glycerol monoalkene diol diethers: a novel series of archaeal lipids detected in hydrothermal environments, *Rapid Commun. Mass Sp.*, 30, 54–602016.

595 Baxter, A. J., Van Bree, L. G. J., Peterse, F., Hopmans, E. C., Villanueva, L., Verschuren, D., and Sinninghe Damsté, J. S.: Seasonal and multi-annual variation in the abundance of isoprenoid GDGT membrane lipids and their producers in the water column of a meromictic equatorial crater lake (Lake Chala, East Africa), *Quaternary Sci. Rev.*, 273, 107263, 2021.

Bebout, B. M., Hoehler, T. M., Thamdrup, B. O., Albert, D., Carpenter, S. P., Hogan, M., Turk, K., and 600 Des Marais, D. J.: Methane production by microbial mats under low sulphate concentrations, *Geobiology*, 2, 87–96, 2004.

Behr, H. J., and Röhricht, C.: Record of seismotectonic events in siliceous cyanobacterial sediments (Magadi cherts), Lake Magadi, Kenya, *Int. J. Earth Sci.*, 89, 268–283, 2000.

Behr, H. J.: Magadiite and Magadi chert: a critical analysis of the silica sediments in the Lake 605 Magadi Basin, Kenya, in *Sedimentation in Continental Rifts* (SEPM Spec. Publ. 73), edited by: Renaut, R.W., and Ashley, G.A., SEPM, Tulsa, 257–273, 2002.

Birgel, D., Meister, P., Lundberg, R., Horath, T. D., Bontognali, T. R., Bahniuk, A. M., de Rezende, C. E., Vasconcelos, C., and McKenzie, J. A.: Methanogenesis produces strong ^{13}C enrichment in stromatolites of Lagoa Salgada, Brazil: a modern analogue for Palaeo-/Neoproterozoic stromatolites? 610 *Geobiology*, 13, 245–266. 2015.

Blaga, C. I., Reichart, G. J., Heiri, O., and Sinninghe Damsté, J. S.: Tetraether membrane lipid distributions in water-column particulate matter and sediments: a study of 47 European lakes along a north–south transect, *J. Paleolimnol.*, 41, 523–540, 2009.

Bligh, E.G., and Dyer, W.J.: A rapid method of lipid extraction and purification, *Can. J. Biochem.*

615 Phys. 37, 911–917, 1959.
Boetius, A., Ravenschlag, K., Schubert, C. J., Rickert, D., Widdel, F., Gieseke, A., Amann, R.

Jørgensen, B.B., Witte, U., and Pfannkuche, O.: A marine microbial consortium apparently mediating anaerobic oxidation of methane, *Nature*, 407, 623–626, 2000.

Casanova., J.: Les Stromatolites Continentaux: Paléoécologie, Paléohydrologie, Paléoclimatologie.
620 Application au Rift Gregory, Thèse Docteur d'Etat-Sciences, Université d'Aix Marseille II, France, 1986.

Casanova, J.: Stromatolites et hauts niveaux lacustres Pléistocènes du basin Natron-Magadi (Tanzanie-Kenya), *Sci. Géol. Bull.*, 40, 135–153, 1987.

Casanova, J., Hillaire-Marcel, C.: Chronologie et paléohydrologie des hauts niveaux quaternaires du 625 basin Natron-Magadi (Tanzanie-Kenya) d'après la composition isotopique (^{18}O , ^{13}C , ^{14}C , U/Th) des stromatolites littoraux, *Sci. Géol. Bull.*, 40, 121–134, 1987.

Cassar, N., Laws, E. A., Bidigare, R. R., and Popp B. N.: Bicarbonate uptake by Southern Ocean phytoplankton, *Global Biogeochem. Cy.*, 18, GB2003, doi:10.1029/2003GB002116, 2004.

Castañeda, I. S., and Schouten, S.: A review of molecular organic proxies for examining modern 630 and ancient lacustrine environments, *Quaternary Sci. Rev.*, 30, 2851–2891, 2011

Cohen, A., Campisano, C., Arrowsmith, R., Asrat, A., Behrensmeyer, A. K., Deino, A., Feibel, C., Hill, A., Johnson, R., Kingston, J., Lamb, H., Lowenstein, T., Noren, A., Olago, D., Owen, R. B., Potts, R., Reed, K., Renaut, R., Schäbitz, F., Tiercelin, J.-J., Trauth, M. H., Wynn, J., Ivory, S., Brady, K., O'Grady, R., Rodysill, J., Githiri, J., Russell, J., Foerster, V., Dommain, R., Rucina, S., Deocampo, 635 D., Russell, J., Billingsley, A., Beck, C., Dorenbeck, G., Dullo, L., Feary, D., Garello, D., Gromig, R., Johnson, T., Junginger, A., Karanja, M., Kimburi, E., Mbuthia, A., McCartney, T., McNulty, E., Muiruri, V., Nambiro, E., Negash, E. W., Njagi, D., Wilson, J. N., Rabideaux, N., Raub, T., Sier, M. J., Smith, P., Urban, J., Warren, M., Yadeta, M., Yost, C., and Zinaye, B.: The Hominin Sites and Paleolakes Drilling Project: inferring the environmental context of human evolution from eastern 640 African rift lake deposits, *Sci. Dril.*, 21, 1–16, <https://doi.org/10.5194/sd-21-1-2016>, 2016.

Crane, K.: Thermal variations in the Gregory Rift Valley of southern Kenya (?), *Tectonophysics* 74, 239–262, 1981.

Damnati., B., and Taieb, M.: Solar and ENSO signatures in laminated deposits from Lake Magadi (Kenya) during the Pleistocene/Holocene transition, *J Afr. Earth Sci.*, 21, 373–382.

645 645 https://doi.org/10.1016/0899-5362(95)00094-A, 1995.

DeMenocal, P., Ortiz, J., Guilderson, T., Adkins, J., Sarnthein, M., Baker, L., and Yarusinsky, M.: Abrupt onset and termination of the African Humid Period: rapid climate responses to gradual insolation forcing, *Quaternary Sci. Rev.*, 19, 347–361, 2000.

Deocampo, D. M., and Renaut, R. W.: Geochemistry of African soda lakes, in *Soda Lakes of East Africa*, edited by: Schagerl, M., Springer, Cham, 77–96, 2016.

650 650 Deocampo, D. M., Owen, R. B., Lowenstein, T. K., Renaut, R. W., Rabideaux, N. M., Billingsley, A., Cohen, A., Deino, A.L., Sier, M.J., Luo, S., Shen, C.-C., Gebregiorgis, D., Campisano, C., and Mbuthia, A., Orbital control of Pleistocene euxinia in Lake Magadi, Kenya, *Geology*, 50, 42–47, 2022.

De Cort, G., Mees, F., Renaut, R. W., Sinnesael, M., Van der Meeran, T., Goderis, S., Keppens, E., Mbuthia, A., and Verschuren, D.: Late-Holocene sedimentation and sodium carbonate deposition in hypersaline, alkaline Nasikie Engida, southern Kenya Rift Valley, *J. Paleolimnol.*, 62, 279–300. 2019.

655 655 de Rosa, M., de Rosa, S., Gambacorta, A., Minale, L., and Bu'lock, J. D.: Chemical structure of the ether lipids of thermophilic acidophilic bacteria of the *Caldariella* group, *Phytochemistry*, 16, 1961–1965, 1977.

Eugster, H. P.: Inorganic bedded cherts from the Magadi area, Kenya, *Contrib. Mineral. Petrol.*, 22, 1–31, 1969.

Eugster, H.P.: Chemistry and origin of the brines of Lake Magadi, Kenya, *Mineral. Soc. Am. Spec. Pap.*, 3, 213–235, 1970.

Eugster, H.P.: Lake Magadi, Kenya and its precursors, in *Hypersaline Brines and Evaporites*, edited by 665 665 Nissenbaum, A., Elsevier, Amsterdam, 195–232, 1980.

Eugster, H.P., and Hardie, L.A., Saline lakes, in *Lakes: Chemistry, Geology, Physics*, edited by Lerman, A., Springer, New York, 237–293, 1978.

Eugster, H.P.: Lake Magadi, Kenya: a model for rift valley hydrochemistry and sedimentation, in *Sedimentation in the African Rifts* (Geol. Soc. Lond. Special Publ. 25), edited by: Frostick, L.E., 670 670 Renaut, R.W., Reid, I., Tiercelin, J.-J., 177–189, 1986.

Fairhead, J. D., Mitchell, J. G., and Williams, L. A. J.: New K/Ar Determinations on rift volcanics of S. Kenya and their bearing on age of rift faulting, *Nature Phy. Sci.*, 238, 66–69, <https://doi.org/10.1038/physci238066a0>, 1972.

Fazi, S., Amalfitano, S., Venturi, S., Pacini, N., Vazquez, E., Olaka, L. A., Tassi, F., Crognale, S., Herzsprung, P., Lechtenfeld, O.J., Cabassi, J., Capecchiacci, F., Rossetti, S., Yakimov, M.M., Vaselli, O., Harper, D.M., and Butturini, A.: High concentrations of dissolved biogenic methane associated with cyanobacterial blooms in East African lake surface water, *Commun. Biol.*, 4, 845, 2021.

Ferland, T., An Evaluation of the Organic Geochemical Potential to Reconstruct Mid-Pleistocene Paleoclimate Adjacent to an Established Hominin Site: Lake Magadi, Kenya (Doctoral dissertation, 680 University of Pittsburgh), 2017.

Freeman, K. H., and Pancost, R.D.: Biomarkers for terrestrial plants and climate, in *Treatise on Geochemistry*, Volume 12, Second Edition, edited by: Holland, H.D., and Turekian, K.K., Elsevier, Amsterdam, 395–416, 2014.

Gallois, R. W., and Cox, B. M., The stratigraphy of the Lower Kimmeridge Clay of eastern England, 685 *Proc. Yorks. Geol. Soc.*, 41, 13–26, 1976.

Giani, D., Giani, L., Cohen, Y., and Krumbein, W. E. (1984). Methanogenesis in the hypersaline Solar Lake (Sinai), *FEMS Microbiol. Lett.*, 25, 219–224.

Goetz, C., and Hillaire-Marcel, C., U-series disequilibria in early diagenetic minerals from Lake Magadi sediments, Kenya: dating potential, *Geochim. Cosmochim. Acta*, 56, 1331–1341. 1992.

690 Grant, W. D., and Jones, B. E., Bacteria, archaea and viruses of soda lakes, in *Soda Lakes of East Africa*, edited by: Schagerl, M., Springer, Cham, 97–147, 2016.

Hardie, L.A., and Eugster, H.P.: The evolution of closed-basin brines, *Mineral. Soc. Am. Spec. Publ.* 3, 273–290, 1970.

Hinrichs K.-U., and Boetius, A.: The anaerobic oxidation of methane: New insights in microbial 695 ecology and biogeochemistry, in *Ocean Margin Systems*, edited by: Wefer, G., Billett, D. Hebbeln, D., Jorgensen, B.B., M. Schlüter, M. T., and van Weering, M.T., Springer, Berlin, Heidelberg, 457–477, 2002.

Hoehler, T. M., Alperin, M. J., Albert, D. B., and Martens, C. S.: Apparent minimum free energy

requirements for methanogenic Archaea and sulfate-reducing bacteria in an anoxic marine sediment,
700 FEMS Microbiol. Ecol., 38, 33–41, 2001.

Hopmans, E. C., Schouten, S., and Sinninghe Damsté, J. S.: The effect of improved chromatography on
GDGT-based palaeoproxies, *Org. Geochem.*, 93, 1–6, 2016.

Inglis, G. N., Farnsworth, A., Lunt, D., Foster, G. L., Hollis, C.J., Pagani, M., Jardine, P. E., Pearson, P.
N., Markwick, P., Galsworthy, A. M. J., Raynham, L., Taylor, K.W.R., and Pancost, R.D.: Descent
705 toward the Icehouse: Eocene sea surface cooling inferred from GDGT distributions, *Paleoceanography*,
30, 1000–1020, <https://doi.org/10.1002/2014PA002723>, 2015.

In 't Zandt, M. H., de Jong, A. E., Slomp, C. P., and Jetten, M. S.: The hunt for the most-wanted
chemolithoautotrophic spookmicrobes, *FEMS Microbiol. Ecol.*, 94, fify064, 2018.

Jaeschke, A., Op den Camp, H. J., Harhangi, H., Klimiuk, A., Hopmans, E. C., Jetten, M. S., Schouten,
710 S., and Sinninghe Damsté, J.S.: 16S rRNA gene and lipid biomarker evidence for anaerobic
ammonium-oxidizing bacteria (anammox) in California and Nevada hot springs, *FEMS Microbiol.
Ecol.*, 67, 343–350, 2009.

Jahnke, L. L., Orphan, V. J., Embaye, T., Turk, K. A., Kubo, M. D., Summons, R. E., and Des Marais,
D.J.: Lipid biomarker and phylogenetic analyses to reveal archaeal biodiversity and distribution in
715 hypersaline microbial mat and underlying sediment, *Geobiology*, 6, 394–410, 2008.

Jetten, M. S., Niftrik, L. V., Strous, M., Kartal, B., Keltjens, J. T., and Op den Camp, H. J.:
Biochemistry and molecular biology of anammox bacteria, *Crit. Rev. Biochem. Mol. Biol.*, 44, 65–84,
2009.

Johannesson, K. H., & Lyons, W. B. (1994). The rare earth element geochemistry of Mono Lake water
720 and the importance of carbonate complexing. *Limnology and Oceanography*, 39(5), 1141-1154.

Johnson, M. S., Matthews, E., Du, J., Genovese, V., and Bastviken, D.: Methane emission from
global lakes: New spatiotemporal data and observation-driven modeling of methane dynamics indicates
lower emissions, *J. Geophys. Res. Biogeosci.*, 127, e2022JG006793, 2022.

Jones, B.J., Eugster, H.P., and Rettig, S.F.: Hydrochemistry of the Lake Magadi basin, Kenya,
725 *Geochim. Cosmochim. Acta* 41, 53–72, 1977

Kambura, A. K., Mwirichia, R. K., Kasili, R. W., Karanja, E. N., Makonde, H. M., and Boga, H. I.:

Bacteria and Archaea diversity within the hot springs of Lake Magadi and Little Magadi in Kenya, BMC Microbiol., 16, 136, <https://doi.org/10.1186/s12866-016-0748-x>, 2016.

Kim, J. H., Van der Meer, J., Schouten, S., Helmke, P., Willmott, V., Sangiorgi, F., Koç, N., Hopmans, 730 E.C., and Sinninghe Damsté, J. S.S.: New indices and calibrations derived from the distribution of crenarchaeal isoprenoid tetraether lipids: Implications for past sea surface temperature reconstructions, Geochim. Cosmochim. Acta, 74, 4639–4654, 2010.

Kim, B., and Zhang, Y. G.: Methane Index: Towards a quantitative archaeal lipid biomarker proxy for reconstructing marine sedimentary methane fluxes, Geochim. Cosmochim. Acta, 354, 74–87, 2023.

735 Knappy, C.S., and Keely, B.J: Novel glycerol dialkanol triols in sediments: transformation products of glycerol dibiphytanyl glycerol tetraether lipids or biosynthetic intermediates? Chem. Commun., 48, 841–843, 2012.

Koga, Y., Nishihara, M., Morii, H., and Akagawa-Matsushita, M.: Ether polar lipids of methanogenic bacteria: Structures, comparative aspects, and biosynthesis, Microbiol. Rev., 57, 164– 740 182. <https://doi.org/10.1128/mr.57.1.164-182.1993>.

Koga, Y., Morii, H.: Recent advances in structural research on ether lipids from Archaea including comparative and physiological aspects, Biochim. Biophys. Acta, 69, 2019–2034. 2005.

Kumar, D. M., Woltering, M., Hopmans, E. C., Sinninghe Damsté, J. S., Schouten, S., and Werne, J. P.: The vertical distribution of Thaumarchaeota in the water column of Lake Malawi inferred from core and 745 intact polar tetraether lipids, Org. Geochem., 132, 37–49. 2019.

Lameck, A. S., Skutai, J., and Boros, E.: Review of chemical properties of inland soda and saline waters in East Africa (rift valley region), J. Hydrol. Reg. Stud., 46, 101323, 2023.

Langworthy, T. A.: Long-chain diglycerol tetraethers from *Thermoplasma acidophilum*, Biochim. Biophys. Acta (BBA) - Lipid Lipid Met., 487, 37–50. 1977.

750 Lee, D. H., Kim, J. H., Lee, Y. M., Stadnitskaia, A., Jin, Y. K., Niemann, H., Kim, Y.-G., and Shin, K. H.: Biogeochemical evidence of anaerobic methane oxidation on active submarine mud volcanoes on the continental slope of the Canadian Beaufort Sea, Biogeosciences, 15, 7419–7433, 2018.

Lee, H., Fischer, T.P., Muirhead, J.D., Ebinger, C.J., Kattenhorn, S.A., Sharp, Z.D., Kianji, G., Takahata, N., Sano, Y., 2017. Incipient rifting accompanied by the release of subcontinental

755 lithospheric mantle volatiles in the Magadi and Natron basin, East Africa. *J. Volcanol. Geotherm. Res.* 346, 118–133.

Leland, H. V., and Berkas, W. R.: Temporal variation in plankton assemblages and physicochemistry of Devils Lake, North Dakota, *Hydrobiologia*, 377, 57–71, 1998.

Lewis, M.L.: Tropical limnology, *Annu. Rev. Ecol. Syst.*, 18, 159–184, 1987.

760 Li, M., Peng, C., Zhu, Q., Zhou, X., Yang, G., Song, X., and Zhang, K.: The significant contribution of lake depth in regulating global lake diffusive methane emissions, *Water Res.*, 172, 115465, 2020.

Liu, Y., and Whitman, W. B.: Metabolic, phylogenetic, and ecological diversity of the methanogenic archaea, *Ann. NY Acad. Sci.*, 1125, 171–189, 2008.

Liu, X.-L., Lipp, J.S., Schröder, J.M., Summons, R.E., and Hinrichs, K.-U.: Isoprenoid glycerol 765 dialkanol diethers: a series of novel archaeal lipids in marine sediments, *Org. Geochem.* 43, 50–55. 2012.

Liu, C., and Wang, P.: The role of algal blooms in the formation of lacustrine petroleum source rocks—evidence from Jiyang depression, Bohai Gulf Rift Basin, eastern China, *Palaeogeogr. Palaeoclimatol., Palaeoecol.*, 388, 15–22, 2013.

770 Marchant, R., Richer, S., Boles, O., Capitani, C., Courtney-Mustaphi, C. J., Lane, P., Prendergast, M. E., Stump, D., De Cort, G., Kaplan, J. O., Phelps, L., Kay, A., Olago, D., Petek, N., Platts, P. J., Punwong, P., Widgren, M., Wynne-Jones, S., Ferro-Vázquez, C., Benard, J., Boivin, N., Crowther, A., Cuní-Sánchez, A., Deere, N.J., Ekblom, A., Farmer, J., Finch, J., Fuller, D., Gaillard-Lemdale, M.-J., Gillson, L., Githumbi, E., Kabora, T., Kariuki, R., Kinyanjui, R., Kyazike, E., Lang, C., Leju, J., 775 Morrison, K.D., Muiruri V., Mumbi, C., Muthoni, R., Muzuka, A., Ndiema, E., Nzabandora, C.K., Iaya Onjala, I., Pas Schrijver, A., Rucina, S., Shoemaker, A., Thornton-Barnett, S., van der Plas, G., Watson, E.E., Williamson, D., Wright, D.: Drivers and trajectories of land cover change in East Africa: Human and environmental interactions from 6000 years ago to present, *Earth-Sci. Rev.*, 178, 322–378, <https://doi.org/10.1016/j.earscirev.2017.12.010>. 2018.

780 Marzi, R., Torkelson, B. E., and Olson, R. K.: A revised carbon preference index, *Org. Geochem.*, 20, 1303–1306, 1993.

Melack, J. M., and MacIntyre, S.: Morphometry and physical processes of East African soda lakes,

in Soda Lakes of East Africa, edited by: Schagerl, M., Springer, Cham, 61–76, 2016.

Meybeck, M.: Global distribution of lakes, in Physics and Chemistry of Lakes, edited by Lerman, S.,

785 Imboden, D.M., and Gat J.L., Springer, Berlin, Heidelberg, 1–35, 1995.

Miller, L. G., Jellison, R., Oremland, R. S., Culbertson, C.W.: Meromixis
in hypersaline Mono Lake, California. 3. Biogeochemical response to stratification and overturn,
Limnol. Oceanogr., 38, 1040–1051, doi: 10.4319/lo.1993.38.5.1040. 1993.

Morii, H., Eguchi, T., Nishihara, M., Kakinuma, K., Konig, H., Koga, Y.: A novel ether core lipid
790 with H-shaped C-80-isoprenoid hydrocarbon chain from the hyperthermophilic methanogen
Methanothermus fervidus, Biochim. Biophys. Acta, 1390, 339–345.1998.

Morrissey, A., Scholz, C. A., and Russell, J. M.: Late Quaternary TEX 86 paleotemperatures from the
world's largest desert lake, Lake Turkana, Kenya, J. Paleolimnol., 59, 103–117, 2018.

Muirhead, J.D., Kattenhorn, S.A., Lee, H., Mana, S., Turrin, B.D., Fischer, T.P., Kianji, G., Dinde, E.,
795 Stamps, D.S.: Evolution of upper crustal faulting assisted by magmatic volatile release during early-
stage continental rift development in the East African Rift. Geosphere 12, 1670–1700. 2016.

Muiruri, V.M., Owen, R.B., Lowenstein, T.K., Renaut, R.W., Marchant, R., Rucina, S.M., Cohen, A.C.,
Deino, A.L., Sier, M.J., Luo, S., Leet, K., Campisano, C., Rabideaux, N.M., Deocampo, D., Shen, C.-
C., Mbuthia, A., Davis, B.C., Aldossari, W., Wang, C.: A million year vegetation history and
800 palaeoenvironmental record from the Lake Magadi Basin, Kenya Rift Valley, Palaeogeogr.,
Palaeoclimatol., Palaeoecol., 567, 110247, 2021.

Nijaguna, B. T.: Biogas Technology, New Age International, New Delhi, 2006.

Norði, K. Á., Thamdrup, B., and Schubert, C. J.: Anaerobic oxidation of methane in an iron-rich
Danish freshwater lake sediment, Limnol. Oceanogr., 58, 546–554, 2013.

805 Oliva, M. G., Lugo, A., Alcocer, J., Peralta, L., and del Rosario Sánchez, M.: Phytoplankton
dynamics in a deep, tropical, hypersaline lake, in Saline Lakes (Publications from the 7th International
Conference on Salt Lakes, Death Valley National Park, California, USA, September 1999), edited by:
Melack, J.M., Jellison, R., and Herbst, D.N., Kluwer, Dordrecht, 299–306, 2001.

Oremland, R. S., Marsh, L. M., and Polcin, S. (1982). Methane production and simultaneous sulphate
810 reduction in anoxic, salt marsh sediments, Nature, 296, 143–145, 1982.

Oren, A., and Garrity, G. M.: Valid publication of the names of forty-two phyla of prokaryotes, *Int. J. Syst. Evol. Microbiol.*, 71, 005056, 2021.

Ortiz, K., Arrowsmith, R., Cohen, A.S., Feibel, C.S., Deino, A., Hill, A., Beck, C.C., Campisano, C.J., Valachovic, J., Kingston, J., 2015, Paleoclimate And Paleoenvironmental Forcing On Early Humans: 815 Loi Analysis Of Three HSPDP Drill Core Sites In Kenya And Ethiopia. *Geological Society of America Ann. Mtg.*, Baltimore, MD

Owen, R. B., Rabideaux, N., Bright, J., Rosca, C., Renaut, R. W., Potts, R., Behrensmeyer, A. K., Deino, A. L., Cohen, A. S., Muiruri, V., Dommain, R.: Controls on Quaternary geochemical and mineralogical variability in the Koora Basin and South Kenya Rift, *Palaeogeogr. Palaeoclim.*

820 Palaeoecol, 637, 111986, 2024.

Owen, R. B., Renaut, R. W., Lowenstein, T. K., Stockhecke, M., Rabideaux, N. M., Leet, K., Cohen, A. S., Scott, J. J., Muiruri, V. M.: Pleistocene stratigraphy and sedimentation in the Magadi-Ewaso Nyiro basins, South Kenya Rift, *Palaeogeogr. Palaeoclim. Palaeoecol.*, 112790, 2024.

Owen, R. B., Renaut, R. W., Muiruri, V. M., Rabideaux, N. M., Lowenstein, T. K., McNulty, E. P., 825 Leet, K., Deocampo, D., Luo, S., Deino, A. L., Cohen, A., Sier, M. J., Campisano, C., Shen, C.-C., Billingsley, A., Mbuthia, A., and Stockhecke, M.: Quaternary history of the Lake Magadi Basin, southern Kenya Rift: Tectonic and climatic controls, *Palaeogeogr. Palaeoclimatol. Palaeoecol.*, 518, 97–118, 2019.

Pancost, R. D., Hopmans, E. C., and Sinninghe Damsté, J. S.: Archaeal lipids in Mediterranean cold 830 seeps: molecular proxies for anaerobic methane oxidation, *Geochim. Cosmochim. Acta*, 65, 1611–1627, 2001.

Parnell, J.: Metal enrichments in solid bitumens: a review. *Min. Deposita*, 23, 191–199. 1988

Paull, C. K., Lorenson, T. D., Borowski, W. S., Ussler III, W., Olsen, K., and Rodriguez, N. M.: Isotopic composition of CH₄, CO₂ species, and sedimentary organic matter within samples from the 835 Blake Ridge: Gas source implications, *Proc. ODP, Sci. Res.*, 164, 67–78, 2000.

Pearson, A., Huang, Z., Ingalls, A. E., Romanek, C. S., Wiegel, J., Freeman, K. H., Smittenberg, R. H., and Zhang, C. L.: Nonmarine crenarchaeol in Nevada hot springs, *Appl. Environ. Microbiol.*, 70, 5229–5237. 2004.

Pearson, A., Pi, Y., Zhao, W., Li, W., Li, Y., Inskeep, W., Perevalova, A., Romanek, C., Li, S., Zhang, C.L.: Factors controlling the distribution of archaeal tetraethers in terrestrial hot springs, *Appl. Environ. Microbiol.*, 74, 3523–3532, 2008.

Pecoraino, G., D’Alessandro, W., and Inguaggiato, S.: The other side of the coin: geochemistry of alkaline lakes in volcanic areas, in *Volcanic Lakes*, edited by: Rouwet, D., Christenson, B., Tassi, F., and Vandemeulebrouck, J., Springer, Berlin, Heidelberg, 219–237, 2015.

Pitcher, A., Rychlik, N., Hopmans, E. C., Spieck, E., Rijpstra, W. I. C., Ossebaar, J., Schouten S., Wagner, M., and Sinninghe Damsté, J. S.: Crenarchaeol dominates the membrane lipids of *Candidatus Nitrososphaera gargensis*, a thermophilic Group I. 1b Archaeon, *ISME J.*, 4, 542–552, 2010.

Rattanasriampaipong, R., Zhang, Y. G., Pearson, A., Hedlund, B. P., and Zhang, S.: Archaeal lipids trace ecology and evolution of marine ammonia-oxidizing archaea, *Proc. Natl. Acad. Sci.*, 119(31), e2123193119, 2022.

Reinhardt, M., Goetz, W., Duda, J. P., Heim, C., Reitner, J., and Thiel, V.: Organic signatures in Pleistocene cherts from Lake Magadi (Kenya) – implications for early Earth hydrothermal deposits. *Biogeosciences*, 16, 2443–2465, 2019.

Renaut, R. W., and Owen, R. B.: *The Kenya Rift Lakes: Modern and Ancient: Limnology and Limnogeology of Tropical Lakes in a Continental Rift*, Springer, Berlin, Heidelberg, 2023.

Rinke, C., Chuvochina, M., Mussig, A. J., Chaumeil, P. A., Davín, A. A., Waite, D. W., Whitman, W.B., Parks, D.H., and Hugenholtz, P.: A standardized archaeal taxonomy for the Genome Taxonomy Database, *Nature Microbiol.*, 6, 946–959, 2021.

Ritchie, J. C., Eyles, C. H., and Haynes, C. V.: Sediment and pollen evidence for an early to mid-Holocene humid period in the eastern Sahara, *Nature*, 314, 352–355, 1985.

Robertson, C. E., Spear, J. R., Harris, J. K., and Pace, N. R.: Diversity and stratification of archaea in a hypersaline microbial mat, *Appl. Environ. Microbiol.*, 75, 1801–1810, 2009.

Rosentreter, J. A., Borges, A. V., Deemer, B. R. , Holgerson, M. A., Liu, S., Song, C., Melack, J., Raymond, P. A., Duarte, C. M., Allen, G. A., Olefeldt, D., Poulter, B., Battin, T. I., and Eyre, B. D.: Half of global methane emissions come from highly variable aquatic ecosystem sources, *Nature Geosci.*, 14, 225–230, <https://doi.org/10.1038/s41561-021-00715-2>, 2021.

Rütters, H., Sass, H., Cypionka, H., and Rullkötter, J.: Phospholipid analysis as a tool to study complex microbial communities in marine sediments, *J. Microbiol. Meth.* 48, 149–160, 2002.

Schagerl, M. (Ed.): *Soda Lakes of East Africa*, Springer, Cham, 2016.

870 Schagerl, M., and Renaut, R. W.: Dipping into the soda lakes of East Africa, in *Soda Lakes of East Africa*, edited by: Schagerl, M., Springer, Cham, 3–34, 2016.

Schouten, S., Hopmans, E. C., Schefuß, E., and Sinninghe Damsté, J. S.: Distributional variations in marine crenarchaeotal membrane lipids: a new tool for reconstructing ancient sea water temperatures? *Earth Planet. Sci. Lett.* 204, 265–274, 2002.

875 Schouten, S., Wakeham, S. G., Hopmans, E. C., and Sinnenhe Damsté, J. S.: Biogeochemical evidence that thermophilic archaea mediate the anaerobic oxidation of methane, *Appl. Environ. Microbiol.*, 69, 1680–1686, 2003.

Schouten, S., Hopmans, E. C., and Sinnenhe Damsté, J. S.: The organic geochemistry of glycerol dialkyl glycerol tetraether lipids: A review, *Org. Geochem.*, 54, 19–61, 2013.

880 Schubotz, F., Meyer-Dombard, D. R., Bradley, A. S., Fredricks, H. F., Hinrichs, K. U., Shock, E. L., and Summons, R. E.: Spatial and temporal variability of biomarkers and microbial diversity reveal metabolic and community flexibility in streamer biofilm communities in the Lower Geyser Basin, Yellowstone National Park, *Geobiology*, 11, 549–569, 2013.

Shah, S. R., Mollenhauer, G., Ohkouchi, N., Eglinton, T. I., and Pearson, A.: Origins of archaeal 885 tetraether lipids in sediments: Insights from radiocarbon analysis, *Geochim. Cosmochim. Acta*, 72, 4577–4594, 2008.

Shanahan, T. M., McKay, N. P., Hughen, K. A., Overpeck, J. T., Otto-Btiesner, B., Heil, C. W., King, J., Scholz, C.A., and Peck, J.: The time-transgressive termination of the African Humid Period, *Nature Geosci.*, 8, 140–144, 2015.

890 Sinnenhe Damsté, J. S., Schouten, S., Hopmans, E. C., Van Duin, A. C., and Geenevasen, J. A.: Crenarchaeol, *J. Lipid Res.*, 43, 1641–1651, 2002.

Sinnenhe Damsté, J. S., Rijpstra, W. I. C., Hopmans, E. C., Jung, M. Y., Kim, J. G., Rhee, S. K., Steglmeier, M., and Schleper, C. (2012). Intact polar and core glycerol dibiphytanyl glycerol tetraether lipids of group I. 1a and I. 1b Thaumarchaeota in soil, *Appl. Environ. Microbiol.*, 78, 6866–6874, 2012.

895 Sikes, N. E.: Early hominid habitat preferences in East Africa: paleosol carbon isotopic evidence, J. Hum. Evol., 27, 25–45, 1994.

Sivan, O., Adler, M., Pearson, A., Gelman, F., Bar-Or, I., John, S. G., and Eckert, W.: Geochemical evidence for iron-mediated anaerobic oxidation of methane, Limnol. Oceanogr., 56, 1536–1544, 2011

Smith, J. M., Green, S. J., Kelley, C. A., Prufert-Bebout, L., and Bebout, B. M.: Shifts in methanogen 900 community structure and function associated with long-term manipulation of sulfate and salinity in a hypersaline microbial mat, Environ. Microbiol., 10, 386–394, 2008.

Sorokin, D. Y., Foti, M., Pinkart, H. C., and Muyzer, G.: Sulfur-oxidizing bacteria in Soap Lake (Washington State), a meromictic, haloalkaline lake with an unprecedented high sulfide content, Appl. Environ. Microbiol., 73, 451–455, 2007.

905 Sorokin, D. Y., Abbas, B., Geleijnse, M., Pimenov, N. V., Sukhacheva, M. V., and van Loosdrecht, M. C.: Methanogenesis at extremely haloalkaline conditions in the soda lakes of Kulunda Steppe (Altai, Russia), FEMS Microbiol. Ecol., 91, fiv016, 2015.

Sturt, H. F., Summons, R. E. Smith, K., Elvert, M. and Hinrichs, K. U.: Intact polar membrane lipids in prokaryotes and sediments deciphered by high-performance liquid chromatography/electrospray 910 ionization multistage mass spectrometry - new biomarkers for biogeochemistry and microbial ecology, Rapid Comm. Mass Spec. 18, 617–28, 2004.

Straka, L. L., Meinhardt, K. A., Bollmann, A., Stahl, D. A., and Winkler, M. K.: Affinity informs environmental cooperation between ammonia-oxidizing archaea (AOA) and anaerobic ammonia-oxidizing (Anammox) bacteria, ISME J., 13, 1997–2004, 2019.

915 Summons, R. E., Franzmann, P. D., and Nichols, P. D.: Carbon isotopic fractionation associated with methylotrophic methanogenesis, Org. Geochem., 28, 465–475, 1998.

Sun, Y., Liu, C., Lin, M., Li, Y., and Qin, P.: Geochemical evidences of natural gas migration and releasing in the Ordos Basin, China, Energy Explor. Exploit., 27, 1–13, 2009.

Talling J. F., and Lemoalle, J.: Ecological Dynamics of Tropical Inland Waters, Cambridge University 920 Press, Cambridge, 1998.

Taylor, K. W., Huber, M., Hollis, C. J., Hernandez-Sanchez, M. T., and Pancost, R. D.: Re-

evaluating modern and Palaeogene GDGT distributions: Implications for SST reconstructions, *Global Planet. Change*, 108, 158–174. 2013.

925 Turich, C., Freeman, K. H., Bruns, M. A., Conte, M., Jones, A. D., Wakeham, S. G.: Lipids of marine Archaea: patterns and provenance in the water-column and sediments, *Geochem. Cosmochim. Acta*, 71, 3272–3291, <https://doi.org/10.1016/j.gca.2007.04.013>, 2007.

Verpoorter, C., Kutser, T., Seekell, D. A., and Tranvik, L. J.: A global inventory of lakes based on high-resolution satellite imagery, *Geophys. Res. Lett.*, 41, 6396–6402, 2014.

930 Volkova, N. I.: Geochemistry of rare elements in waters and sediments of alkaline lakes in the Sasykkul depression, East Pamirs, *Chem. Geol.*, 147, 265–277, 1998.

Wakeham, S. G., Lewis, C. M., Hopmans, E. C., Schouten, S., and Sinninghe Damsté, J. S.: Archaea mediate anaerobic oxidation of methane in deep euxinic waters of the Black Sea, *Geochim. Cosmochim. Acta*, 67, 1359–1374. 2003.

Weijers, J. W., Lim, K. L., Aquilina, A., Sinninghe Damsté, J. S., and Pancost, R. D.:
935 Biogeochemical controls on glycerol dialkyl glycerol tetraether lipid distributions in sediments characterized by diffusive methane flux, *Geochem., Geophys., Geosyst.*, 12, <https://doi.org/10.1029/2011GC003724>, 2011.

Werne, J. P., Zitter, T., Haese, R. R., Aloisi, G., Bouloubassi, I., Heijs, S., Fiala-Medioni, A., Pancost, R.D., Sinninghe Damsté, J. S., de Lange, G., Forney, L.J., Gottschal, J.C., Foucher, J.-P., Masclé, J.,
940 Woodside, J., and the MEDINAUT and MEDINETH Shipboard Scientific Parties: Life at cold seeps: A synthesis of ecological and biogeochemical data from Kazan mud volcano, eastern Mediterranean Sea, *Chem. Geol.*, 205, 367–390, 2004.

Williamson, D., Taieb, M., Damnati, B., Icole, M., and Thouveny, N.: Equatorial extension of the Younger Dryas event: rock magnetic evidence from Lake Magadi (Kenya), *Global Planet. Change*, 7, 235–242, 1993.

945 Woulds, C., Bell, J. B., Glover, A. G., Bouillon, S., Brown L.S.: Benthic carbon fixation and cycling in diffuse hydrothermal and background sediments in the Bransfield Strait, Antarctica, *Biogeosciences* 17, 1–12, <https://doi.org/10.5194/bg-17-1-2020>. 2020.

Wright, H. E.: A square-rod piston sampler for lake sediments, *J. Sediment. Petrol.*, 37, 975–976, 1967.

950 Wright H. E.: Cores of soft lake sediments, *Boreas*, 9, 107–114. <https://doi.org/10.1111/j.1502-3885.1980.tb01032.x>., 1980.

Wynn, J. G., Lowenstein, T. K., Renaut, R. W., Owen, R. B. and McNulty, E. P.: Superheavy pyrite formation in hypersaline lakes of East Africa: a paleosalinity proxy for Lake Magadi HSPDP cores, *Geol. Soc. Am. Abstr. Progr.*, 50, Paper 184–3, <https://doi.org/10.1130/abs/2018AM-323852>, 2018.

955 Xia, L., Cao, J., Hu, W., Stüeken, E. E., Wang, X., Yao, S., Zhi, D., Tang, Y., Xiang, B., and He, W.: Effects on global warming by microbial methanogenesis in alkaline lakes during the Late Paleozoic Ice Age (LPIA), *Geology*, 51, 935–940, 2023.

Zhang, Y. G., Zhang, C. L., Liu, X. L., Li, L., Hinrichs, K. U., and Noakes, J. E.: Methane Index: A tetraether archaeal lipid biomarker indicator for detecting the instability of marine gas hydrates, *Earth 960 Planet. Sci. Lett.*, 307, 525–534, 2011.

Zhuang, G. C., Elling, F. J., Nigro, L. M., Samarkin, V., Joye, S. B., Teske, A., and Hinrichs, K. U.: Multiple evidence for methylotrophic methanogenesis as the dominant methanogenic pathway in hypersaline sediments from the Orca Basin, Gulf of Mexico. *Geochim. Cosmochim. Acta*, 187, 1–20. 2016.

965

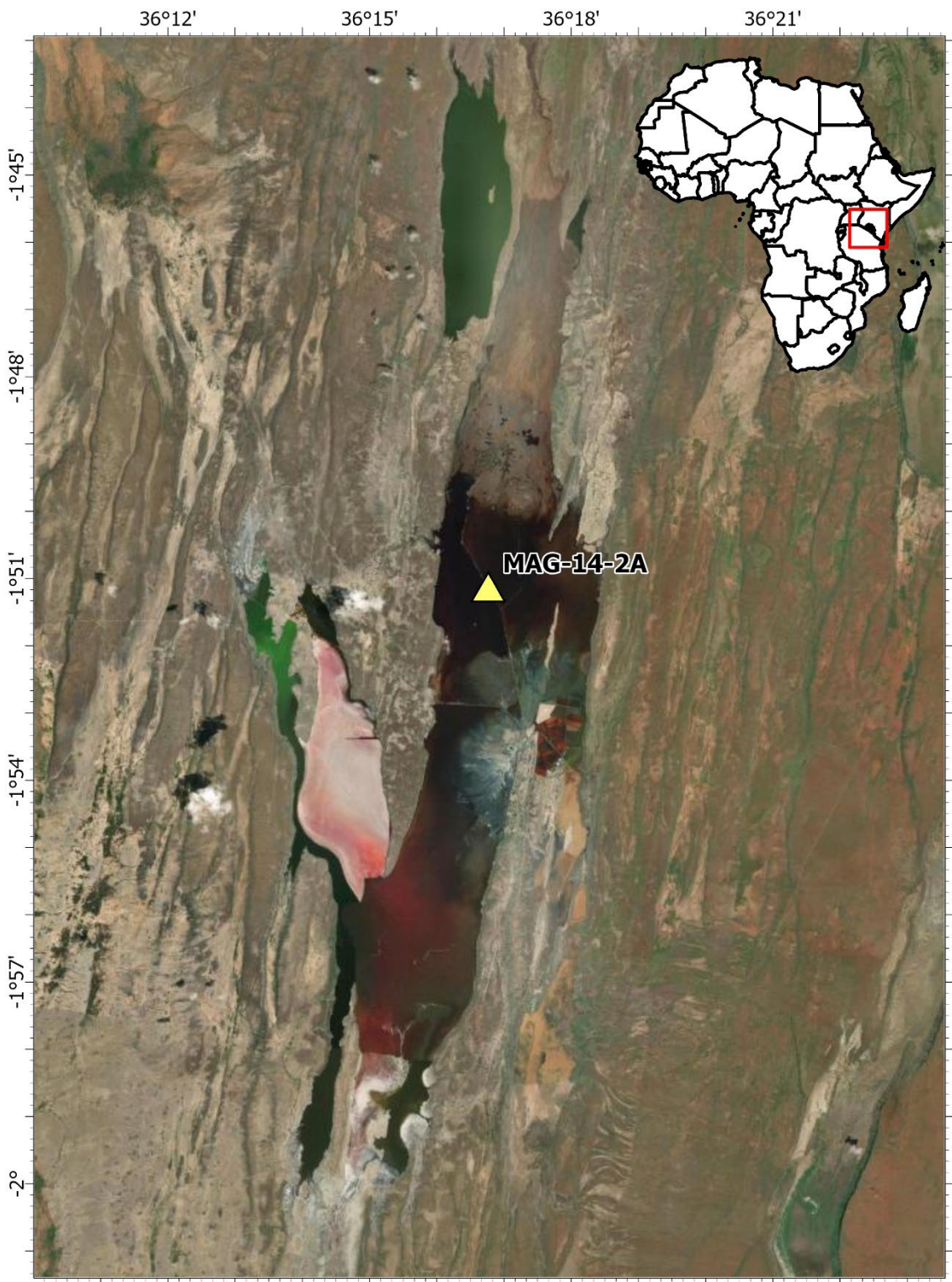


Figure 1. Map of the drilling location of MAG-14-2A (yellow triangle) in Lake Magadi for the Hominin
970 Sites and Paleolakes Drilling Project (HSPDP).

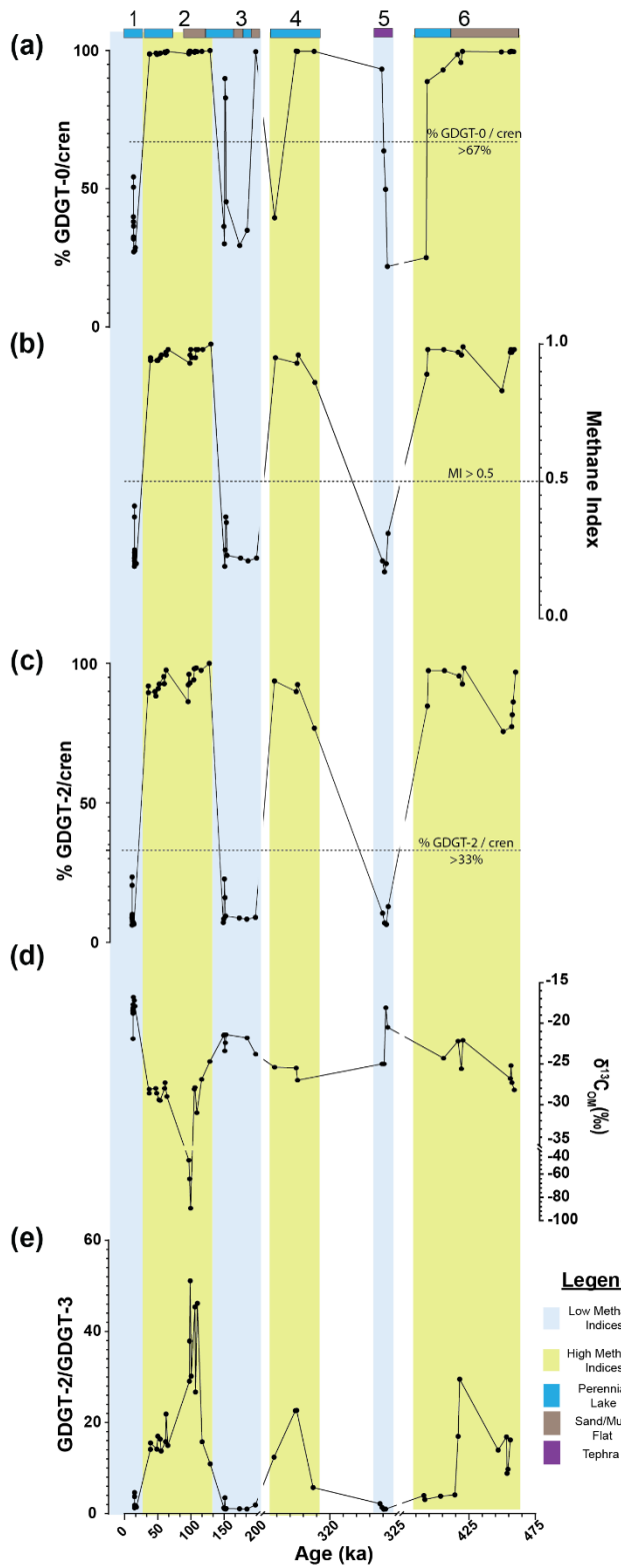
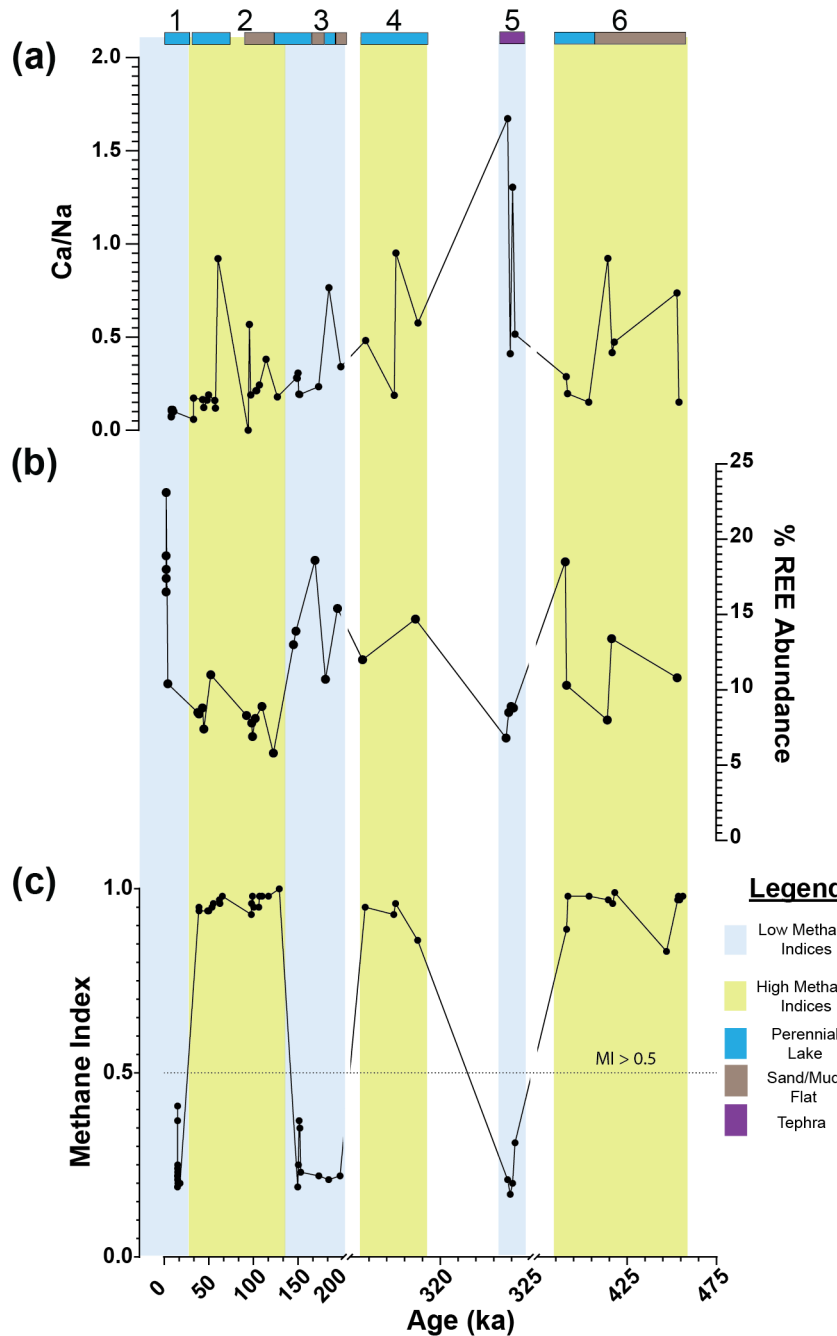


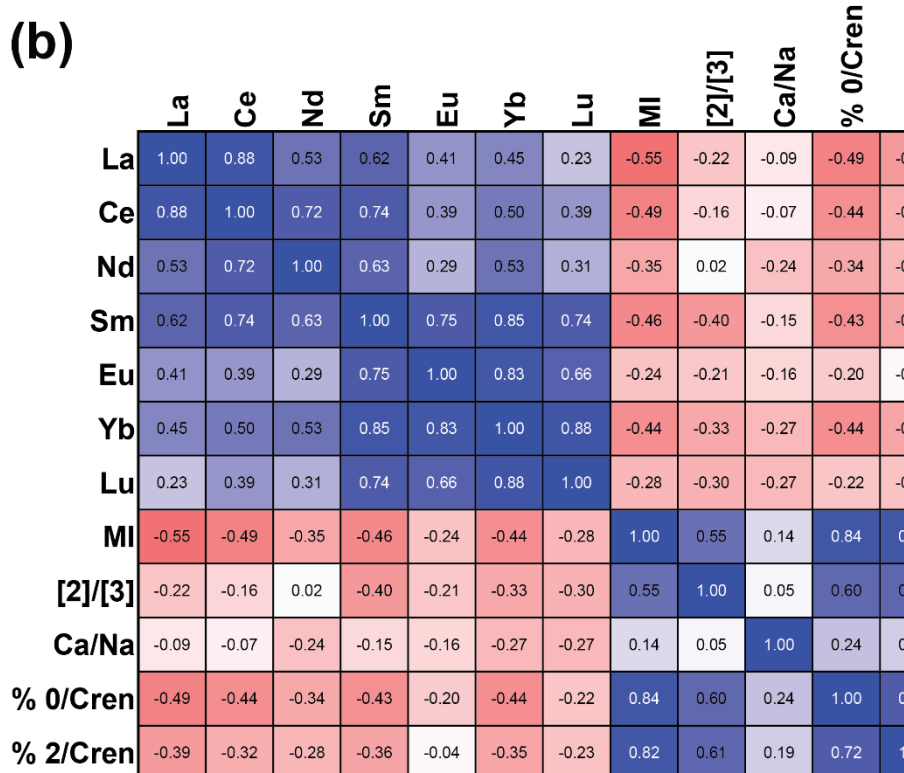
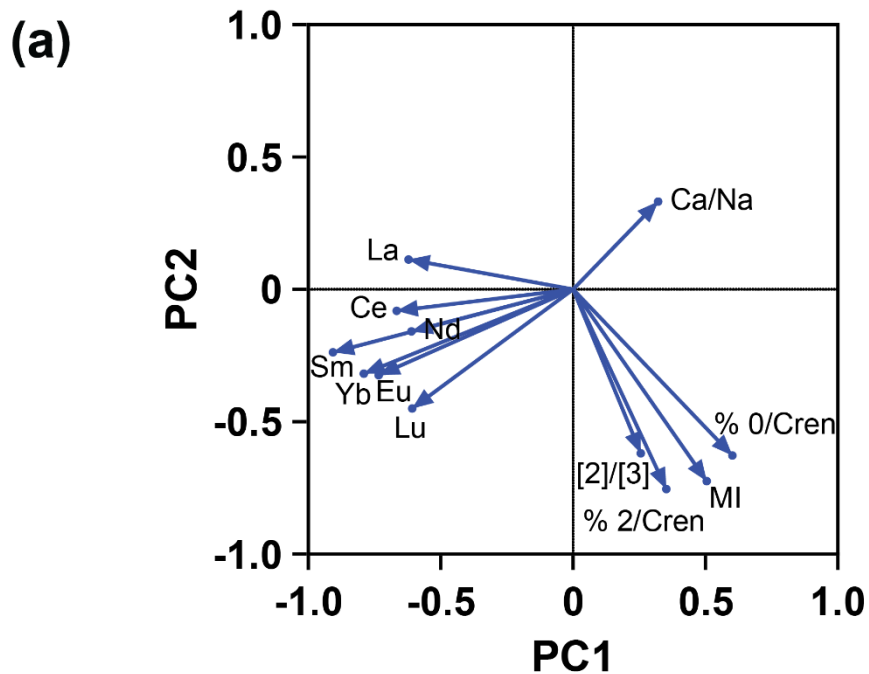
Figure 2. Downcore variations in Lake Magadi of the **a)** % 0/Cren, **b)** MI, **c)** % 2/Cren, **d)** bulk $\delta^{13}\text{C}_{\text{OM}}$, and **e)** the GDGT-2/GDGT-3 ([2]/[3]) values from ca. 14.9 to 456 ka. Sections 1, 3, and 5 are low MI intervals outlined in blue, the high MI intervals in Sections 2, 4, and 6 are in yellow. Bands at the top of the graph indicate the inferred (via Renaut and Owen, 2023) lake levels and major inputs with dark blue indicating a perennial lake, brown indicating a sand or mud flat, and purple indicating tephra. Dotted lines on each section denote the cut-off points for methane related indices MI (>0.5), %GDGT-2/cren ($>33\%$), and %GDGT-0 / cren ($>67\%$). See Section 2.3.2 for more details. Note the breaks in the X-axis scale.

975

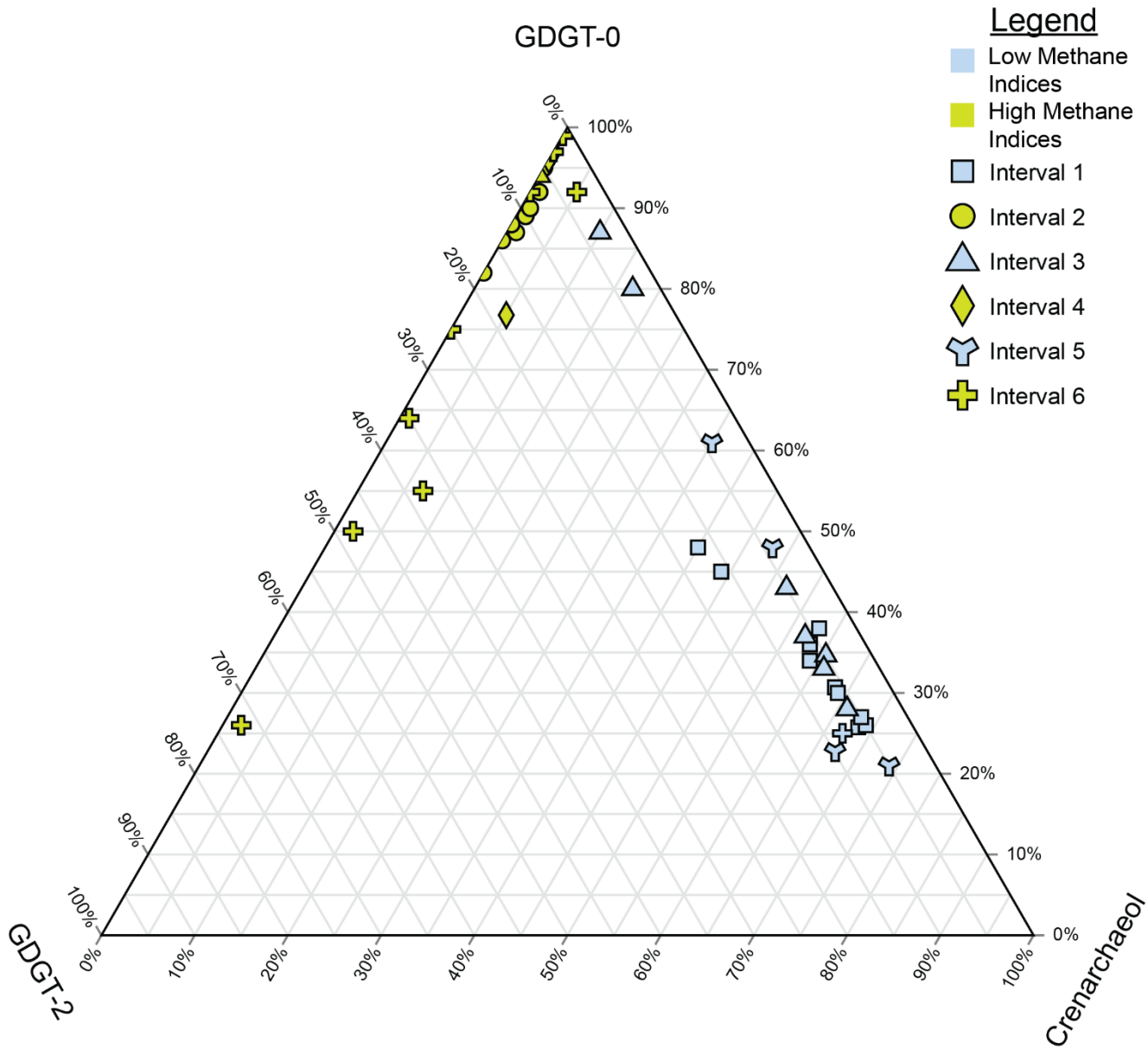


980 **Figure 3.** Downcore plot for Lake Magadi of **a)** Ca/Na, **b)** %REE abundance, and **c)** MI. Values range from ca. 14.9 to 456 ka and Sections 1, 3, and 5 are outlined in blue reflecting a low MI interval, while high MI intervals are outlined in yellow. Bands at the top of the graph indicate the inferred (via Renaud and Owen, 2023) lake levels and major inputs with dark blue indicating a perennial lake, brown indicating

a sand or mud flat, and purple indicating tephra. The dotted line on the MI plot (c) denotes the cutoff point
985 >0.5 for values significantly affected by methane cycling archaea. Note the breaks in the X-axis scale and
in the Y-axis scale for the $\delta^{13}\text{C}_{\text{OM}}$. REE values are from Owen et al. (2019).



990 **Figure 4.** Both **a)** PCA and **b)** Spearman Correlation Matrix showing the relationship between methane related indices (MI and [2] / [3]) and REEs (La, Ce, Nd, Sm, Eu, Tb, Yb, and Lu) in the sampled intervals of the core. A negative relationship is seen between the methane indices and REEs as shown by opposing eigenvectors on the PCA **(a)** and negative r values on the correlation matrix **(b)**. REE values are from Owen et al. (2019).



995 **Figure 5.** Ternary plot of crenarchaeol, GDGT-0, and GDGT-2, which are used to calculate the methane indices. Samples are split by both their interval (denoted by their shape) and whether they are from a high MI (yellow) or low MI (blue) interval. Higher proportions of GDGT-0 indicate methanogenic inputs, higher GDGT-2 indicate methanotrophy, and higher crenarchaeol indicates more mesophilic conditions influenced by hot springs.

1000